ASTRONOMY & ASTROPHYSICS
SUPPLEMENT SERIES

Astron. Astrophys. Suppl. Ser. **59**, 369-397 (1985)

Spectrophotometry of peculiar B and A stars. XVII. 63 Andromedae, HD 34452, Epsilon Ursae Majoris, CQ Ursae Majoris, CU Virginis, CS Virginis and Beta Coronae Borealis

D. M. Pyper ([1],*) and S. J. Adelman ([2],*,**)

([1]) Department of Physics, University of Nevada, Las Vegas, Las Vegas, NV 89154, U.S.A.
([2]) Department of Physics, The Citadel, Charleston, SC 29409, U.S.A.

Received July 25, accepted September 21, 1984

Summary. — Optical region spectrophotometry results are presented for seven Ap stars. Additional data for two silicon stars, HD 34452 and CU Vir, show that both have energy distributions that can be fit by a single global model atmosphere, except for the λ4200 and λ5200 broad absorption features. These features are strong in HD 34452 and show no evidence of variation, while they are weak in CU Vir but show clear evidence of variations. The energy distributions of the five cooler Ap stars cannot be fit by a single model atmosphere. CQ UMa, CS Vir and β CrB all show complicated variations with phase at different wavelengths. Their energy distributions show combined effects of flux redistribution and differential line blanketing. Except for ε UMa, none of these five stars show evidence of variations of the λ4200 or λ5200 broad absorption features.

Key words : photometry — spectrophotometry — stars : peculiar A — stars : atmospheres of.

1. Introduction.

This paper examines optical region spectrophotometry of seven magnetic Ap stars which cover a considerable range of temperature : 63 And, HD 34452, ε UMa, CQ UMa, CU Vir, CS Vir and β CrB. Table I summarizes the spectrum, photometric and magnetic data that are available for these stars. Even the hottest Ap magnetic stars show evidence of the λ5200 broad absorption feature. Only two stars, ε UMa and CU Vir, clearly show variations of this feature with phase. The two cooler stars that are also strong spectrum variables, CQ UMa and CS Vir, have complex light variations with phase. The energy distributions of all the stars studied here show differences from those of solar abundance model atmospheres.

The data reduction techniques and those for forming the various indices have been discussed in Paper I (Adelman, 1979), Paper III (Adelman and Pyper, 1979), Paper IV (White *et al.*, 1980) and Paper XIII (Pyper and Adelman, 1983) of this series. Table II contains the journal of observations while table III compares the synthesized *u-b* and *b-y* values and those of D.M.P. (this paper) with those given in the literature. Table IV contains the new four-color and Hβ-photometry, while in table V we compare the temperatures obtained by various authors with those determined from our data. Tables VI through XII give the energy distributions and synthesized indices for the seven stars of this paper. The model atmospheres used for comparison with Ap star energy distributions are fully line blanketed solar composition models calculated with the ATLAS program (Kurucz, 1979). Unless otherwise indicated, $\log g = 4.0$ was used. The theoretical Strömgren colors based on those models calculated by Kurucz (1979) are given by Relyea and Kurucz (1978).

Most of the observations were obtained with the HCO Scanner on the No. 1 92-cm telescope at Kitt Peak National Observatory (KPNO). A few scans of β CrB and ε UMa were made with the Cassegrain Scanner on the 1.5-m telescope at Palomar Observatory and the 1.5-m telescope at Mt. Wilson Observatory (MWO).

2. 63 Andromedae.

Winzer (1974) found that 63 And (HR 682 = HD 14392) was a moderately large amplitude photometric variable ($0^m.05$ in U). The ephemeris is

$$\mathrm{JD}(U_{max}) = 2441619.66 + 1.3040\,E.$$

There is a dip in the U, B and V light curves near phase 0.8 which needs to be confirmed.

(*) Visiting Astronomer, Kitt Peak National Observatory, National Optical Astronomical Observatories, operated by the Association of Universities for Research in Astronomy, Inc., under contract with the National Science Foundation.

(**) Observations were also made with the 1.5-m telescope at Palomar Observatory, which is operated jointly with the California Institute of Technology and the Carnegie Institution of Washington, and with the 1.5-m telescope of Mt. Wilson Observatory of the Carnegie Institution of Washington.

We obtained nine scans of 63 And, the first eight of which were taken in the same observing run. In figure 1, we have plotted our synthesized values of *u-b* and *b-y* and the absorption feature indices as well as the ΔU-ΔB and ΔB-ΔV values from Winzer (1974). It is difficult to compare our values with those of Winzer, as our coverage is less complete. The values of scan 9, which are plotted using a different symbol than those of the other scans, appear to be shifted or in error. The bandpasses used to obtain it are two-thirds as wide as those for the other scans. If the scan 9 values are shifted by about 0.3 cycle compared to those of scans 1-8, then the period may be $1^d.3103$. Thus, the values of scans 1-8 can be used to show relative variability, but their relation to the *UBV* photometry is somewhat uncertain.

Examination of the $\Delta\imath$, $\Delta\imath^*$, $\Delta\imath^{**}$, Δa and $\Delta a'$ values plotted as a function of phase shows definite to suggested variability, in phase with one another (Fig. 1). Additional data are needed to confirm these results after a better period is determined. The average values of $\Delta\imath$ and $\Delta\imath^{**}$ suggest marginal presence of the λ4200 feature and the average value of $\Delta\imath^*$ suggests presence. The values for individual scans range between those indicating absence and presence for all three indices. The average Δa value suggests that the λ5200 feature is just present, and the average $\Delta a'$ value suggests marginal presence, with the individual values for both indices ranging from those indicating absence to presence. This is an unusual occurrence for the Ap stars but it is somewhat similar to the results for 56 Ari (Adelman, 1983, Paper XIV) and for CU Vir (see Sect. 6).

The average energy distribution (Fig. 2) shows a weak λ4200 feature and a shallow but definite λ5200 feature in accord with the average values of the feature indices. The λ5200 feature exhibits a slight minimum at 5200 Å. The λ4464 value is above the trend of adjacent values in the Paschen continuum. The Balmer continuum is featureless and there is no sign of a λ6300 feature.

If we proceed as in other papers in this series and use the *u-b* values to predict the temperature, we find it corresponds to a normal stellar atmosphere whose tempeperature is 12800 K. Comparison of the Balmer jump with models shows it is fit by the predictions of a 12900 K atmosphere. However, longward of 4255 Å, the model values tend to be systematically fainter than the observations when the Balmer jump is fit. Fitting the Paschen continuum alone requires a 10750 K model, however, the λ4464 value falls above the predictions of this model. These values are cooler than the previously published temperature estimates given in table V.

3. HD 34452.

Adelman and White (1980) in Paper VI presented spectrophotometry of HD 34452 (HR 1732). The nine MWO scans had 16 bandpasses each while the three KPNO scans had 28 bandpasses each. The data suggested that *u-b* was probably variable with an amplitude of $0^m.02$ and further that Deutsch's (1947) period of $2^d.4660$ was probably nearly correct. The λ5200 broad absorption feature was very strong with a sharp core near λ5200.

To confirm and to extend the results of that study, ten additional scans were obtained at KPNO with a total of 47 bandpasses each. As some bandpasses such as the one centered at λ4032 are affected by He I lines, new bandpasses were selected in the nearby continuum. The average energy distribution (Fig. 3) shows more details than were previously seen. The values of the MWO scans in the ultraviolet were omitted from the calculation of the average energy distribution due to the difficulties with these values (discussed in Paper VI). There is a definite λ4200 broad absorption feature along with the strong λ5200 feature whose central portion extends from $\lambda\lambda$4975 to 5700. Further, there may be a secondary minimum near λ5470. The faintness of the λ6370 and λ6440 magnitudes relative to adjacent continuum values suggests the possibility of a broad absorption feature near λ6400. When allowance is made for the variability and differences in coverage of the period, the new average energy distribution is in reasonable agreement with that of Paper VI (see Table III). The new Paschen continuum has a slightly different slope, as evidenced also in *b-y*, which changed from $-0^m.116$ (Paper VI) to $-0^m.125$ (this paper).

Recent four-color photometric data of HD 34452 by D.M.P. (Table IV), compared with the previous photometry by Rakos (1962) (Fig. 4), are best fit by a period with the ephemeris

$$\mathrm{JD0} = 2437295.88 + 2.4662\,E,$$

which also fit the $m(\lambda)$ *vs.* phase variations

$$(m(\lambda) = m(5000) - 2.5\log(F_\lambda/F_{5000}))$$

of White (Paper VI). The spectrum variations of He I estimated by Deutsch (1947) are not inconsistent with this period (e.g., primary *y* maximum = He I minimum as in CU Vir). Figure 5 shows the indices plotted as a function of phase for the ten new scans and the three KPNO scans from Paper VI. The *b-y* and *u-b* data show evidence of a small amplitude variation with phase but because of greater scatter, systematic variations of Δa, $\Delta\imath$, and $\Delta\imath^*$ cannot be seen. The evidence for the variation of $\Delta a'$ is more convincing but requires further confirmation. No evidence for cyclic variations in Hβ is shown by the β index, the *h* index of Paper VI or the *hb* index (defined in Paper XIII) of scans 13-22. Part of the differences between the *b-y*, *u-b* and Δa values of the three 28 bandpass scans and those for the ten new scans may be due to differences in the coverage of the Paschen continuum.

The average *u-b* color corresponds to that of a 15800 K model atmosphere. Indeed the predictions of a 15800 K model atmosphere fit the Balmer continuum, the Balmer jump and the Paschen continuum outside of the broad absorption features. These temperatures are 50 K higher than those given in Paper VI. Comparison of the predictions and the observed values confirms the presence of a weak continuum absorption feature near λ6400 and indicates that the λ5200 feature wings may extend from 4785 to 5840 Å (Fig. 3).

4. Epsilon Ursae Majoris.

The CrSr star ε UMa is the brightest Ap star and has been extensively studied spectroscopically. Some of the more recent investigations (Woszczyk and Jasiński, 1980; Tektunali, 1981, and references therein) confirm that the star is a mild spectrum variable. The period is about five

days and the primary ions involved are Ca II and Cr II, which vary out of phase with each other. Line doubling is seen at phases 0.3 and 0.7, and other profile variations are also present. The line width is relatively large, with $v \sin i = 35$ km s^{-1} (Preston, 1970). Because of this, Babcock (1958) was unable to measure a magnetic field for ε UMa. Borra and Landstreet (1980) find the magnetic field to be smaller than 100 G. The abundances of Fe and Ti are normal, while Sr, Cr, Mn, Y, Zr, Ba and the REE are overabundant and Al, Si and Ca underabundant (Tektunali, 1981).

Previous photoelectric photometry by Provin (1953) shows a small amplitude variation with a possible double curve in the yellow and blue magnitudes and the same period reported by Guthnick (1931). Provin's ephemeris is

$$\text{JD(Ca II min)} = 2434131.124 + 5.0887\,E,$$

which we use here. Ultraviolet photometry (Molnar, 1975; Mallama and Molnar, 1977) shows variations in antiphase with those of Provin, with the maximum amplitude at λ1430 and the « null wavelength » at about 3300 Å.

Our observations include spectrophotometry in 1972-74 and 1981 (Table II). The average values of the λ5200 and λ4200 indices and the average energy distribution (Table VIII, Fig. 2) show weak to moderate strength broad absorption features with little substructure. There is little or no general depression in the blue-violet region of the Paschen continuum. The temperatures obtained by previous investigators are summarized in table V. Our average synthesized *u-b* color (Table VIII) corresponds to a model having $T_{\rm eff} = 9120$ K if $\log g = 4.0$ or 9370 K if $\log g = 3.5$. Our average energy distribution is best matched in the red Paschen continuum by a 9500 K model and the values in the immediate vicinity of the Balmer jump by a 9000 K model (Fig. 2). The best overall fit is by a 9500 K, $\log g = 3.0$ model (9400 K, $\log g = 3.5$ fits almost as well). These lower $\log g$ values agree with the Balmer line profiles we obtained for ε UMa. They will be discussed in more detail in a subsequent paper.

When the indices are plotted *vs.* phase (Fig. 6), *b-y* shows little evidence of variation for either the synthesized spectrophotometric values or the four-color photometry, while *u-b* varies with an amplitude of about $0^{m}.025$ and is reddest at about phase 0.6. Figure 7 shows that this variation is principally in the ultraviolet. The Δ*a* and Δ*a*′ indices both show evidence of variation with maxima at primary *y* maximum. There are differences in both indices between the values of scans 1-18 and 19-29 which are due to differences in wavelength coverage and probably also in width of bandpasses. Figure 7 shows that the magnitudes relative to *m*(5000) are fainter in the region λλ4800-5500 at phase 0.0 compared to phase 0.6, while the maximum in Δ*ι* and Δ*ι** at phase 0.7 (Fig. 6) appears to be due to *m*(4464) and *m*(4255) being brighter at this phase; however, there is more absorption in the range λλ4200-4500 at phase 0.0 compared to phase 0.6. The four-color photometry of D.M.P. (Table IV, Fig. 8) agrees with the photometry of Provin (1953) and the variation of scans 1-18 and 23 relative to η UMa ($\Delta m(\lambda) = m(\lambda)_{\rm star} - m(\lambda)_{\rm comp.}$), except that the spectrophotometric values of Δ*m*(5556) and Δ*m*(4255) do not show a double minimum. Mallama and Molnar (1977) predict a « null wavelength » at about λ3540; however, the *u* and Δ*m*(3509) values vary in phase with *y* and Δ*m*(5556), which is also the case for Δ*m*(3448) and Δ*m*(3390). Therefore the « null wavelength » must occur between λ3390 and λ2460, where Molnar (private communication) found a variation in antiphase to *y*. The photometric β index shows a slight variation with phase (Fig. 8) with a maximum at about phase 0.5 (Ca II K maximum). Similar variations are also seen in the equivalent widths of Hγ through H8 measured by Woszczyk and Michalowski (1981).

5. CQ Ursae Majoris.

This SrCrEu star (Cowley *et al.*, 1969) was first noted as having strong Sr lines by Bidelman (1965). Burke and Howard (1972) and Winzer (1974) who did *UBV* photometry of CQ UMa (HR 5153 = HD 119213), found periods near $1^{d}.7$. Wolff and Morrison (1975) reported their four-color data were better fit by a period near $2^{d}.451$, although a period twice this length was not ruled out. Mikulášek *et al.* (1978), comparing their *UBV* photometry with that of Burke *et al.*, gave the ephemeris

$$\text{JD(max. light)} = 2440747.620 + 2.44997\,E,$$

with an uncertainty of $0^{d}.00002$, but were not able to eliminate the $4^{d}.9$ period. The $2^{d}.45$ period was established as correct by Pavlovski (1979); the radial velocity data (Mikulášek, 1981) and the four-color photometry of Wolff and Morrison and D.M.P. (this paper, Table IV) are also fit by this period. A period of $2^{d}.45$ is compatible with the $v \sin i$ values of 30 km s^{-1} and 33 km s^{-1} found by Mikulášek and Grygar (1978) and Glagolevskij *et al.* (1981), respectively. Pavlovski (1979) determined a radius of 2.23 $R_{\odot}$ for CQ UMa. Bonsack (1974) found the Ca II and Cr II lines to be strongly variable and those of Sr II and Mg II possibly variable. The maximum strength of Cr II coincides with maximum light in *b*, *v* and *u* (Wolff and Morrison, 1975). Mikulášek (1978) found that Sr and Fe vary in phase with Cr, while Ti and Eu vary out of phase with them. Glagolevskij *et al.* (1981) measured a large, variable, reversing magnetic field with a large scatter (Table I); the amplitude of the variations may vary with the ion. Mikulášek (1981) fits the observations to an ORM that has a Eu-Ti spot near the north magnetic pole and a Cr-Sr spot near the south magnetic pole, with Fe concentrated along the magnetic equator.

Our spectrophotometry was carried out in 1973-74 and 1981 at KPNO. The average energy distribution (Fig. 2) and the average values of the broad absorption feature indices (Table IX) show a weak λ4200 and a moderate λ5200 feature, the latter having a sharp core, although not as sharp as that of HD 34452. These features were also detected by Mikulášek (1978), who examined the *UBV*, four-color and ten-color photometry of CQ UMa. The entire blue end of the Paschen continuum ($\lambda < 5700$ Å) is depressed relative to the red Paschen continuum, an effect also seen in a number of other Ap stars (Paper XIII). Our average synthesized value of *u-b* (Table IX) corresponds to a 9570 K model atmosphere. The red end of the Paschen continuum and the slope of the Balmer continuum can be matched by a 8650 K model but the values in the immediate vicinity of the Balmer jump are fit by a 10250 K model.

The four-color and ten-color photometry (Wolff and Morrison, 1975; Mikulášek, 1978; D.M.P. this paper) show little variation in the range $\lambda\lambda$5200-5500, and a maximum amplitude of variation near 4100 Å (Fig. 9). Mikulášek also reports an antiphase variation in the red end of the Paschen continuum and at about 3300 Å, with respect to the blue Paschen continuum. The spectrophotometric values of $\Delta m(\lambda)$ (CQ UMa-HR 5169) for our scans 1-11 show the minimum amplitude of variation occurring near λ5556 and the maximum amplitude at λ4032. The variations of $m(\lambda)$ with phase for scans 12-22 can thus be approximated by plotting $m(\lambda) - m(5556)$, which is done in figure 9. The light curves for $\lambda > 6000$ Å have a double maximum at phases 0.0 and 0.5, while the ultraviolet curves show a flat minimum. Figure 7 shows the energy distributions relative to λ5556 at the two phases of maximum difference in our synthesized *b-y*. The red end of the Paschen continuum ($\lambda > 5500$ Å) is matched to a slightly hotter model atmosphere at phase 0.9 (9000 K) than at phase 0.4 (8750 K), while the entire region 3300 Å $< \lambda <$ 3700 Å varies in phase with the blue end of the Paschen continuum. The β values of D.M.P. and the *hb* values of scans 12-22 show evidence of variation with a maximum at about phase 0.8 and an amplitude of about $0^m.03$ but the scatter is large. The variations of our synthesized *u-b* and *b-y* values correspond to those measured in four-color photometry by Wolff and Morrison (1975) and D.M.P. (Fig. 10), except for zero point shifts. The only absorption feature index that shows clear evidence of variation is $\Delta a'$, which displays a maximum at about phase 0.9. This is probably due to the variation of the « continuum » with phase; the $m(5263)$ value does not change with respect to the $m(5840)$ value during the cycle but the index $m(4785) - m(5840)$ varies in phase with $\Delta a'$. The λ4200 indices not only do not appear to vary with phase but the $\Delta\imath$ and $\Delta\imath^{**}$ indices show absence or only marginal presence at most phases (Fig. 10). The variations of the « λ4100 depression » reported by Mikulášek (1978, 1981) are due to the larger amplitude variation of this region relative to other wavelength regions, not to the variation of the λ4200 absorption feature as defined in this series of papers.

6. CU Virginis.

In paper IV, thirty-one spectrophotometric observations of CU Vir (HR 5313 = HD 124224) were presented. As most of these scans had only a relatively small number of bandpasses and as there were systematic differences in the ultraviolet measurements of the various authors, additional scans were obtained to show further details in the optical energy distribution. The new scans agree in the ultraviolet with the previous measurements of Pyper and Adelman. The problems inherent in using the Cassegrain scanner on the MWO 1.5-m telescope for measurements in the ultraviolet could not be completely corrected by White. The data for the Paschen continuum are apparently not affected by these problems. Thus, for the new average scan, we have omitted White's MWO values in the ultraviolet.

The new scans show that the Paschen continuum, aside from the broad absorption features and the Balmer lines, is in general quite smooth (Fig. 3). The λ4464 value is above the trend of adjacent values in the Paschen continuum but this may be due in part to the presence of the λ4200 feature. The values near λ6300 show a slight depression relative to a continuum drawn through nearby longward and shortward values. The minimum of the λ5200 feature, whose extent is probably from 4975 Å to 5556 Å, is near λ5232. The average values of $\Delta\imath^*$, Δa and $\Delta a'$ indicate definite presence of the relevant features, while the value of $\Delta\imath$ indicates only marginal presence. This is in accord with the spectrophotometry, which shows weak λ4200 and λ5200 features.

The *u-b* and *b-y* values plotted as a function of phase (Fig. 11) follow the trends of those for the previous scans (except for the *u-b* values from MWO scans) and the four-color values of D.M.P. (this paper, Table IV). The variability of *b-y* is definitely confirmed. The new scans show variations in both Δa and $\Delta a'$, although the latter index shows a larger scatter. The variability of the λ5200 feature is also seen in the smaller amplitude of variation of $m(5263)$ compared to $m(5556)$ and $m(4566)$ (Fig. 12). Both the $\Delta\imath$ and $\Delta\imath^*$ values suggest that the λ4200 feature is variable. The variability of the Δa, $\Delta a'$ and $\Delta\imath^*$ indices appears to be roughly in phase. The index values for the most part are greater than the appropriate criterion of presence, but for some scans they are less than those of marginal presence. Near phase 0.9, CU Vir, according to the feature indices, is a normal star. However, if one carefully examines the spectrophotometry there are still subtle differences compared with normal stars that have similar optical region colors.

The new four-color photometry agrees with that of Weiss *et al.* (1976) and the *UBV* photometry of Hardie (1958) as far as can be determined. There is a stronger indication of a double maximum light curve in *b* and *v* in the more recent data, in agreement with $m(\lambda)$ and $\Delta m(\lambda)$ values from scans 1-9 and 21-29 in Paper IV (Fig. 12). The β index shows a similar amplitude of variation to that of Weiss *et al.* The *h* index of Paper IV and the *hb* index of scans 32-49 show similar variations.

The average *u-b* value indicates a temperature of 13100 K, as was found in Paper IV. Also as before, the spectrophotometry matches the predictions of a 13000 K atmosphere outside of the broad absorption features. The λ5200 feature extends from 4975 Å to 5556 Å and there is evidence for a weak λ6300 feature.

7. CS Virginis.

This SrCrEu star is an outstanding magnetic and spectrum variable and has been studied by many investigators. Deutsch (1958) constructed the first ORM for CS Vir (HR 5355 = HD 125248), based on his spectrum variations and the magnetic field measurements of Babcock (1951, 1958). The REE and Fe lines vary 180° out of phase with those of Sr and Cr in a period of about $9^d.295$, the most extreme variations being in the Eu II and Cr II lines. The REE maximum occurs at $H_{\rm eff}$ minimum. These results agree with those of Hockey (1969) and Bonsack (1974). Borra and Landstreet (1980) also constructed an ORM based on their photometrically measured $H_{\rm eff}$ values; the Deutsch and the Borra and Landstreet models both used $v \sin i = 7$ km s^{-1} and the $9^d.3$ period and obtained small values of *i* (Table I). However, the magnetic geometries of the models are quite dissimilar due to the

different assumptions made concerning the structure of the magnetic field and the different methods used to measure $H_{\rm eff}$. As the distributions of metal ions are not identical to those of hydrogen atoms in the atmospheres of Ap stars, magnetic field measurements of lines of different species sample the magnetic field in different ways. This needs to be accounted for in producing an improved ORM. Radial velocity measurements show the star to be a spectroscopic binary. Abt and Snowden (1973) summarized the orbital calculations and state that Deutsch's orbit with $P = 1618^{d}0$ is probably the most accurate.

Babcock (1960) gave a revised period for CS Vir with the ephemeris

$$\mathrm{JD}(H_{\rm eff}\ \mathrm{max.}) = 2430143.07 + 9.2954\,E.$$

This period was also found to fit the *UBV* photometry of Maitzen and Rakosch (1970), the four-color photometry of Wolff and Wolff (1971) and D.M.P. (this paper) and the photometry of Maitzen and Moffat (1972). Blanco *et al.* (1978) suggest a slightly shorter period of $9^{d}.29477$ based on their three-color photometry. Unfortunately, they did not publish a journal of observations or their values. Due to the relatively long period of this star and since the bulk of the photometry was done in the period 1969-71, it cannot be said that the period of Blanco *et al.* better fits the data than the period published by Babcock. The photometry of D.M.P. is not extensive enough to discriminate between the two periods, thus we will use the Babcock period for comparison purposes. All photometry reveals a double maximum light curve in *V* or *y*, with principal maximum at about phase 0.0 and secondary maximum at about phase 0.5. The four-color data (Wolff and Wolff, 1971; Maitzen and Moffat, 1972) show that the primary maximum in *y* becomes the secondary maximum in *b*, the maximum amplitude of variation ($0^{m}.13$) occurs in *v*, which shows an almost sinusoidal variation, and *u* has an amplitude of about $0^{m}.08$ with a hint of the secondary maximum at about phase 0.0.

Our spectrophotometry was obtained in 1972-74 and 1981 at KPNO. The average energy distribution (Fig. 2) shows a moderate λ4200 feature and a strong λ5200 feature, which agrees with the average values of the spectrophotometric indices (Table XI). These features were previously detected by Maitzen and Moffat (1972) and Hardorp (1976). The magnitudes at $\lambda\lambda$6300, 6370 and 6440 are slightly depressed relative to those of the surrounding wavelengths, suggesting the presence of a λ6300 absorption feature. As is the case for the stars discussed in Paper XIII, and CQ UMa (Sect. 5), the blue-violet end of the Paschen continuum suffers a general depression shortward of about 5000 Å. In the Balmer continuum, the 3540 Å magnitude appears relatively bright. Our average synthesized *u-b* color (Table XI) matches that of a 10100 K model atmosphere. When the average energy distribution is compared with model atmospheres, the red end of the Paschen continuum matches a 9675 K model, which also fits the Balmer continuum. However, the values in the immediate vicinity of the Balmer jump are matched by a 10375 K model.

The light variations of CS Vir are complex, as was noted by Wolff and Wolff (1971), Maitzen and Moffat (1972) and Hardorp (1976). As is the case for HD 51418 (Paper XIII) and CQ UMa, the shape of the Paschen continuum varies with phase, the wavelengths shortward of about 5000 Å becoming fainter relative to those to the red (Fig. 7). This behavior also occurs in the Balmer continuum; in CS Vir (as in CQ UMa) the slope appears to remain constant. The values of $\Delta m(\lambda)$ (CS Vir – HR 5332) from scans 3-10 show almost no variation at λ5840. Thus we have combined the $\Delta m(\lambda)$ or the $m(\lambda) - m(5840)$ values from our scans with the photometric data of Wolff and Wolff, Maitzen and Moffat and D.M.P. (Fig. 13). We see a double-maximum light curve for $\lambda > 4600$ Å, however, only in the range $\lambda\lambda$5240-5556 is the maximum at phase 0.0 greater than that at phase 0.5. For $\lambda < 5000$ Å, the maximum at phase 0.5 increases in amplitude to about λ4032, where it is a maximum, then decreases for $\lambda < 3636$ Å. This latter behavior is similar to that of CQ UMa. The β index measured by D.M.P. and the *hb* index for scans 11-14 show a possible variation (Fig. 13); this is in agreement with the Balmer line variations found by Pilachowski and Bonsack (1975).

There is no clear evidence of variation in the λ4200 or λ5200 indices (Fig. 14). The apparent maximum near phase 0.5 for the $\Delta\imath$** index is probably due to the variation in the blue-violet « continuum » with phase. The variation of the « λ4100 depression » reported by Maitzen and Moffat is due to the large amplitude of variation at this wavelength relative to the other parts of the continuum, not to a variation of the λ4200 feature. Both the *u-b* and *b-y* synthesized indices vary in agreement with the four-color indices determined by Wolff and Wolff (1971), Maitzen and Moffat (1972) and D.M.P.

8. Beta Coronae Borealis.

Beta CrB (HR 5747 = HD 137909) is one of the brightest of the cooler Ap stars, classified as CrSrEu. The spectrum is very sharp-lined, with $v \sin i = 3$ km s^{-1} (Preston, 1971). Lines of Sr II and Eu II are prominent while Mg II λ4481 is rather weak (Babcock, 1958). It is a suspected spectrum variable (see, e.g., Stencel and Cowley, 1975; Glagolevskij *et al.*, 1978), but the variations are weak, if present. Abundance analyses (Adelman, 1973 and references therein) show that the iron peak elements are significantly enhanced, with many REE showing even greater enhancement factors. Neubauer (1944) found β CrB to be a spectroscopic binary with a period of 10.496 years. It is possibly a triple system (Neubauer, 1944; Kamper, 1981).

Preston and Sturch (1967) studied the magnetic variations and established the period of variability as

$$\mathrm{JD\ (positive\ crossover)} = 2434217.50 + 18.487\,E.$$

This ephemeris has been confirmed by more recent studies (Borra and Landstreet, 1980). Resolved Zeeman patterns of a few lines with anomalous patterns are seen on very high dispersion spectrograms (Preston, 1969). The mean surface magnetic field has an amplitude of 800 gauss and varies in a single wave with the same period as the effective field.

Observations in the Strömgren system by Wolff and Wolff (1971) show that the *v* magnitude has the largest

amplitude, $0^m.035$, with *u*, *b* and *y* amplitudes about half this value. The minimum in *v* coincides with minimum longitudinal magnetic field. The variations in all four colors are probably in phase, which is also indicated by the *UBV* photometry of Brodskaya (1970) and Burke *et al.* (1970) and four-color measurements by Wolff and Wolff (1971) and D.M.P. (this paper).

Our spectrophotometry was carried out at KPNO, MWO and Palomar Observatories. For the average scan, the synthesized values of *u-b* and *b-y* agree well, when compared with previously published values (Table III). There is no convincing evidence for cyclic variations of any of the indices, *u-b*, *b-y*, Δa, $\Delta a'$, $\Delta\imath$, or $\Delta\imath^*$, when they are plotted *versus* phase (Fig. 15). The *u-b* and *b-y* indices measured by Wolff and Wolff (1971) and D.M.P. also show very little variation with phase. Examination of the spectrophotometric indices for individual scans shows that the values measured by the two authors with different systems (Table II) exhibit systematic differences. These are probably mainly due to differences in the placement and number of spectrophotometric bandpasses for the synthesized indices. However, since the blue region of the spectrum of β CrB is heavily blanketed (Wolff, 1967; Adelman *et al.*, 1981) and presumably very irregular, bandpass width, centering errors and scattered light (seeing) may also cause systematic differences.

The average values of the spectrophotometric indices (Table XII) indicate the presence of a weak λ4200 absorption feature (two indices indicate absence, one, presence) and a moderate λ5200 absorption feature (both indices indicate presence), which is confirmed by inspection of the average flux distribution (Fig. 2). The λ4200 feature may be due to differential line absorption, as the line blanketing coefficients measured by Wolff (1967) show large values in this spectral region. Although our spectrophotometry shows a dip at λ4200, Wolff's results do not show a larger value of the blanketing specifically at this wavelength. However, there is a large uncertainty in Wolff's values because the blanketing coefficients in heavily line blanketed regions, such as the blue end of the Paschen continuum, depend crucially on the placement of the continuum. The average energy distribution also shows a rather sharp dip near λ5263. This is not shown in Wolff's line blanketing measurements although the blanketing coefficients are generally large in the region $\lambda\lambda$4875-5325. In this region one has to be careful in measuring line blanketing coefficients as the spectral sensitivities of most photographic emulsions are definite functions of wavelength. Changes in the continuum level of a few percent due to a broad continuum feature can easily be overlooked.

Effective temperatures and gravities have been estimated by a number of authors; some recent values are given in table V. Our *u-b* value is greater than that of any $\log g = 4.0$ model atmosphere with somewhat similar colors. If we fit to the predictions of $\log g = 3.5$ model atmospheres, the $T_{\rm eff} = 8900$ K. Our average flux distribution, however, cannot be fit by the predictions of a single $\log g = 4.0$ or 3.5 model atmosphere. The red end of the Paschen continuum can be fit by an 8000 K model (Fig. 2), but our measured Balmer jump does not match that of the model. Varying the temperatures or $\log g$ of the model only worsens the fit. Probably in this case, the large amount of blanketing apparent in the blue-violet region has carried over into the near ultraviolet. We note that the Balmer jump of an 8000 K, $\log g = 4.0$ model will fit our observations if the blue end of the Paschen continuum is fit to the $\lambda\lambda$4032-4255 region as shown in figure 2. A 10000 K model will crudely match the Balmer jump when fitted in this way, but the slope of the Balmer continuum is better fit by the 8000 K model.

In figure 16 we show as a function of phase $\Delta m(\lambda)$ (scans 1-16, comparison star = γ CrB) or $m(\lambda) - m(5556)$ (scans 17-30) for various wavelengths along with four-color magnitudes from Wolff and Wolff (1971) and D.M.P. Also included for comparison purposes are the phase variations of the effective longitudinal magnetic fields and the surface magnetic field (Wolff and Wolff, 1970; Borra and Landstreet, 1980). The values from scans 29 and 30 were observed at a substantially different epoch from the rest of the spectrophotometric data but they provide no consistent evidence that the period of variability used is in need of revision. Systematic differences are seen at certain wavelengths and are probably due to the causes discussed above for those of the indices. The variations at $\lambda\lambda$4255-4566 appear to be out of phase with those at λ3571 and perhaps also those at λ6370. As can be seen, the largest variations take place in the region $\lambda\lambda$4032-4566. Since the *u*, *b* and *y* filters all include wavelength regions where the relative variations are small, the variations in *u-b* and *b-y* are small as observed. The variability at λ3571 and possibly λ6370 have extrema roughly in phase with those of H_s, but are phase shifted with respect to those of the longitudinal magnetic field. However, the variations of *y*, *b* and the $\Delta m(\lambda)$ values at $\lambda\lambda$4255, 4464 and 4566 have minima in phase with that of the longitudinal magnetic field.

9. Discussion.

Additional observations of the hot silicon stars HD 34452 and CU Vir confirm that each of their energy distributions are globally fit by a single solar abundance $\log g = 4.0$ model, 15800 K and 13000 K, respectively. The strong λ5200 feature of HD 34452 shows structure and a λ6300 feature is present. On the other hand, in CU Vir these features are weak, with the λ4200 and λ5200 features probably variable. In fact, the energy distribution of CU Vir appears almost normal at λ5200 minimum. These two stars illustrate the extremes in the strength of the broad absorption features seen in the silicon stars. Although both of these stars are helium variables, only in CU Vir, which is also a silicon variable and has variable Hβ, is there any evidence for variability of the broad absorption features. The four-color brightness variations of CU Vir are much greater than in HD 34452.

Epsilon UMa is the only Ap star studied by us in which the Balmer jump is definitely matched by a cooler temperature $\log g = 4.0$ model than is the red end of the Paschen continuum. The average energy distribution and the Hγ and Hα profiles both satisfactorily match models having $\log g = 3.5$, which agrees with the results of previous investigations (see Table V). There are also large amplitude flux variations in the far ultraviolet that are in antiphase with the much smaller variations in the visual wavelengths. As the spectrum variations of ε UMa in the visual region are not large, the far ultraviolet variations may be caused by changes in the continuous opacity rather than variable line

blanketing. This star will be a good candidate for modeling when better laboratory analyses of the Fe peak elements become available. Epsilon UMa also shows evidence for variations of the λ4200 and λ5200 broad absorption features and in Hβ. These variations approximately match the variations in equivalent width of the Balmer lines measured by Woszczyk and Michalowski (1981).

The other stars studied here, 63 And, CQ UMa, CS Vir and β CrB all show behavior typical of the majority of Ap stars, in that their Paschen continua match models with cooler temperatures than do their Balmer jumps. This is demonstrated by figure 17, in which the energy distribution of the silicon star CU Vir is compared to those of 63 And and CS Vir. It is seen that the Balmer jump of 63 And matches that of CU Vir (13000 K) while the red end of its Paschen continuum ($\lambda\lambda$4900-7850) matches that of CS Vir (9800 K). CQ UMa, CS Vir and β CrB all show a general depression of flux relative to the model continua for $\lambda\lambda$4000-4800. For CS Vir, the amount of the depression is a maximum at the phase of REE maximum and Cr minimum line strength, when the *b*, *v* and *u* magnitudes are at maximum brightness. Although there is disagreement between authors as to whether the REE are variable in CQ UMa, in general the relationships are the same as for CS Vir (Fig. 7). As in the case of HD 51418 (Paper XIII) these variations must be due to a combination of differential line blanketing in this spectral region plus flux redistribution from the far ultraviolet. Not enough laboratory analyses are available at present to determine what elements are primarily responsible for the far ultraviolet absorption. No variations in the λ4200 and λ5200 feature indices can be determined separately from the continuum variations.

In the case of β CrB, several problems are seen regarding the variability. Most of the brightness variations appear to be in the continuum in the region $\lambda\lambda$4255-4566 (Fig. 16). These variations are roughly in phase with the $H_{\rm eff}$ variations but both are phase-shifted with respect to the $H_{\rm s}$ variations (Wolff and Wolff, 1970). The implication is that near phase 0.3 we see one pole (positive $H_{\rm eff}$) closest to the sub-earth point and near phase 0.8 the second pole (negative $H_{\rm eff}$) is in that position. This suggests that the absorption near λ4464 is located near the negative pole. However, the variations in the ultraviolet and possibly at $\lambda > 6000$ Å vary more in phase with $H_{\rm s}$. The explanation may lie in how the photospheric intensity depends on the magnetic intensity (see also Adelman *et al.*, 1981).

Acknowledgements.

We would like to express our gratitude to Kitt Peak National Observatory for use of its facilities and to the Citadel Development Foundation and the University of Nevada for financial support for this study.

References

Abt, H. A., Snowden, M. S. : 1973, *Astrophys. J. Suppl.* **25,** 137.
Abt, H. A., Chaffee, F. H., Suffolk, G. : 1972, *Astrophys. J.* **175,** 779.
Adelman, S. J. : 1973, *Astrophys. J.* **183,** 95.
Adelman, S. J. : 1979, *Astron. J.* **84,** 857 (Paper I).
Adelman, S. J. : 1983, *Astron. Astrophys. Suppl. Ser.* **51,** 511 (Paper XIV).
Adelman, S. J., Pyper, D. M. : 1979, *Astron. J.* **84,** 1726 (Paper III).
Adelman, S. J., White, R. E. : 1980, *Astron. Astrophys. Suppl. Ser.* **42,** 289 (Paper VI).
Adelman, S. J., Boyim, B. A., Pyper, D. M., Shore, S. N. : 1981, *Upper Main Sequence CP Stars* (23rd Liège International Astrophys. Coll.) p. 109.
Babcock, H. W. : 1951, *Astrophys. J.* **114,** 1.
Babcock, H. W. : 1958, *Astrophys. J. Suppl.* **3,** 141.
Babcock, H. W. : 1960, *Stellar Atmospheres,* vol. **VI** : « *Stars and Stellar Systems* », ed., J. L. Greenstein, p. 282.
Bidelman, W. P. : 1965, *Vistas Astron.* **8,** 53.
Blanco, C., Catalano, F. A., Strazzula, G. : 1978, *Astron. Astrophys. Suppl. Ser.* **31,** 205.
Bonsack, W. K. : 1974, *Publ. Astron. Soc. Pacific* **86,** 408.
Borra, E. F., Landstreet, J. D. : 1980, *Astrophys. J. Suppl.* **42,** 421.
Borra, E. F., Vaughn, A. H. : 1977, *Astrophys. J.* **216,** 462.
Brodskaya, E. S. : 1970, *Astron. Zh.* **47,** 662.
Burke, E. W., Howard, J. T. : 1972, *Astrophys. J.* **178,** 491.
Burke, E. W., Rolland, W. W., Boy, W. R. : 1970, *J. Roy. Astron. Soc. Canada* **64,** 353.
Cameron, R. C. : 1966, *Georgetown Obs. Monogr.,* No. 21.
Cowley, A., Cowley, C., Jaschek, M., Jaschek, C. : 1969, *Astron. J.* **74,** 375.
Crawford, D. L., Barnes, J. V. : 1969, *Astron. J.* **74,** 407.
Crawford, D. L., Barnes, J. V., Faure, B. Q., Golson, J. C. : 1966, *Astron. J.* **71,** 709.
Crawford, D. L., Barnes, J. V., Gibson, J., Golson, J. C., Perry, C. L., Crawford, M. L. : 1972, *Astron. Astrophys. Suppl. Ser.* **5,** 109.
Deutsch, A. J. : 1947, *Astrophys. J.* **105,** 283.
Deutsch, A. J. : 1952, *Astrophys. J.* **116,** 536.
Deutsch, A. J. : 1958, *IAU Symposium,* No. **6,** p. 209.
Engin, S. : 1976, *Physics of Ap Stars, IAU Coll.* **32,** Vienna, ed., W. W. Weiss, H. Jenkner and H. J. Wood, p. 343.
Glagolevskij, Yu. V., Kozlova, K. I., Polosukhina, N. S. : 1978, *Soviet Astron.-AJ (Lett.)* **4,** 73.
Glagolevskij, Yu. V., Romanyuk, I. I., Kozlova, K. I., Bychkov, V. D., Lebedev, V. S. : 1981, *Communication Special Astrophys. Obs.,* No. 32 (Acad. Nauk, USSR) p. 26.
Grönbech, B., Olsen, E. H. : 1976, *Astron. Astrophys. Suppl. Ser.* **25,** 213.
Guthnick, S. : 1931, *Sitz. Preuss. Akad. Berlin,* No. 27.

HARDIE, R. H. : 1958, *Astrophys. J.* **127,** 606.
HARDORP, J. : 1976, *Physics of Ap Stars, IAU Coll.* **32,** Vienna, ed., W. W. Weiss, H. Jenkner and H. J. Wood, p. 627.
HARDORP, J., SHORE, S. N. : 1971, *Publ. Astron. Soc. Pacific* **83,** 605.
HOCKEY, M. S. : 1969, *Monthly Notices Roy. Astron. Soc.* **142,** 543.
JOHANSEN, K. T., GYLDENKERNE, K. : 1970, *Astron. Astrophys. Suppl. Ser.* **1,** 165.
KAMPER, K. : 1981, private communication.
KURUCZ, R. L. : 1979, *Astrophys. J. Suppl. Ser.* **40,** 1.
LANDSTREET, J. D., BORRA, E. F. : 1977, *Astrophys. J. Lett.* **212,** L43.
MAITZEN, H. M., MOFFAT, A. F. J. : 1972, *Astron. Astrophys.* **16,** 385.
MAITZEN, H. M., RAKOSCH, K. D. : 1970, *Astron. Astrophys.* **7,** 10.
MALLAMA, A. D., MOLNAR, M. R. : 1977, *Astrophys. J. Suppl.* **33,** 1.
MEGESSIER, C. : 1971, *Astron. Astrophys.* **10,** 332.
MIHALAS, D., HENSHAW, J. L. : 1966, *Astrophys. J.* **144,** 25.
MIKULÁŠEK, Z. : 1978, *Publ. Astron. Inst. Czech. Acad. Sci.,* No. **54,** ed. J. Grygar and Z. Mikulášek, p. 22.
MIKULÁŠEK, Z. : 1981, *Communication Special Astrophys. Obs.* No. **32** (Acad. Nauk., USSR) p. 42.
MIKULÁŠEK, Z., GRYGAR, J. : 1978, *Hvar. Obs. Bull.,* No. **2,** 1.
MIKULÁŠEK, Z., HARMANEC, P., GRYGAR, J., ZDARSKY, F. : 1978, *Bull. Astron. Inst. Czech.* **29,** 44.
MOLNAR, M. R. : 1975, *Astrophys. J.* **80,** 137.
NEUBAUER, F. J. : 1944, *Astrophys. J.* **99,** 134.
PAVLOVSKI, K. : 1979, *Astron. Astrophys.* **76,** 364.
PERRY, C. L. : 1969, *Astron. J.* **74,** 139.
PILACHOWSKI, C. A., BONSACK, W. K. : 1975, *Publ. Astron. Soc. Pacific* **87,** 221.
PRESTON, G. W. : 1969, *Astrophys. J.* **158,** 1081.
PRESTON, G. W. : 1970, *Stellar Rotation,* ed. A. Slettebak (Reidel, Holland) p. 254.
PRESTON, G. W. : 1971, *Astrophys. J.* **164,** 309.
PRESTON, G. W., STURCH, C. : 1967, *Magnetic and Related Stars,* ed. R. C. Cameron, p. 111.
PROVIN, S. S. : 1953, *Astrophys. J.* **118,** 489.
PYPER, D. M., ADELMAN, S. J. : 1983, *Astron. Astrophys. Suppl. Ser.* **51,** 365 (Paper XIII).
RAKOS, K. D. : 1962, *Lowell Obs. Bull.* **5,** 227.
RELYEA, L. J., KURUCZ, R. L. : 1978, *Astrophys. J. Suppl.* **37,** 45.
SHALLIS, M. J., BLACKWELL, D. E. : 1979, *Astron. Astrophys.* **79,** 48.
STENCEL, R. E., COWLEY, C. R. : 1975, *Publ. D. A. O.* **14,** 305.
STOKES, N. R. : 1972, *Monthly Notices Roy. Astron. Soc.* **160,** 155.
TEKTUNALI, H. G. : 1981, *Astrophys. Space Sci.* **77,** 41.
WARREN, W. H., Jr. : 1973, *Astron. J.* **78,** 192.
WEISS, W. W., ALBRECHT, R., WEIDER, R. : 1976, *Astron. Astrophys.* **47,** 423.
WHITE, R. E., PYPER, D. M., ADELMAN, S. J. : 1980, *Astron. J.* **85,** 836 (Paper IV).
WINZER, J. E. : 1974, Ph. D. thesis, Univ. of Toronto.
WOLFF, S. C. : 1967, *Astrophys. J. Suppl.* **15,** 21.
WOLFF, S. C., BONSACK, W. K. : 1972, *Astrophys. J.* **176,** 425.
WOLFF, S. C., MORRISON, N. D. : 1975, *Publ. Astron. Soc. Pacific* **87,** 231.
WOLFF, S. C., WOLFF, R. J. : 1970, *Astrophys. J.* **160,** 1049.
WOLFF, S. C., WOLFF, R. J. : 1971, *Astron. J.* **76,** 422.
WOSZCZYK, A., JASIŃSKI, M. : 1980, *Acta Astron.* **30,** 331.
WOSZCZYK, A., MICHALOWSKÍ, T. : 1981, *Acta Astron.* **31,** 339.

TABLE I. — *Summary of spectrum, photometric and magnetic data.*

Star	i	Spectrum Variations	Photometric Amplitude (mag.)	Magnetic Amplitude (kG)	References[3]
63 And	57°	absent?	0.05 (U)	<200 G	a; none; b; c
HD 34452	70°	moderate to large (He I)	0.06 (b)	probable magnetic field	d; e; f, g; c
ε UMa	90°	small (CaII, CrII)	0.03 (b)	<100 G	d; h, i; j, g; c
CQ UMa	40°	large (CaII, CrII)	0.10 (v)	3.25	k; l, m; n, g; o
CU Vir	30°	large (SiII, HeI)	0.14 (u)	1.2	p; p; g; q
CS Vir	11°-30°[1]	large (CrII, REE)	0.13 (v)	3.4	r; c, r; s, t; r
β CrB	19°	small or absent	0.035 (v)	1.1-1.7[2]	u; v, w; s; x, y

Notes: 1) From ORM's; others are calculated from v_e = 162/P (Preston 1970).
2) H_s amplitude is 0.8 kG (Preston 1969).
3) References to columns 2-5, respectively, are separated by ";". The references are:

a) Abt, et al. (1972)
b) Winzer (1974)
c) Borra and Landstreet (1980)
d) Preston (1970)
e) Deutsch (1947)
f) Rakos (1962)
g) D.M.P., this paper
h) Woszczyk and Jasiński (1980)
i) Tektunali (1981)
j) Provin (1953)
k) Pavlovski (1978)
l) Bonsack (1974)
m) Mikulášek (1978)
n) Wolff and Morrison (1975)
o) Glagolevskij, et al. (1981)
p) Deutsch (1952)
q) Landstreet and Borra (1977)
r) Deutsch (1958)
s) Wolff and Wolff (1971)
t) Maitzen and Moffat (1972)
u) Preston (1971)
v) Stencel and Cowley (1975)
w) Glagolevskij, et al. (1978)
x) Wolff and Bonsack (1972)
y) Borra and Vaughn (1977)

TABLE II. — *Journal of observations.*

Star	Scan No.	JD(Hel.) 2440000+	Phase[1]	Observatory	Observer[2]	Bandpass[3] (Å)
63 And	1	4569.663	0.272	Kitt Peak	SJA	30
	2	4569.736	0.328	Kitt Peak	SJA	30
	3	4570.596	0.988	Kitt Peak	SJA	30
	4	4570.651	0.030	Kitt Peak	SJA	30
	5	4570.721	0.083	Kitt Peak	SJA	30
	6	4572.589	0.516	Kitt Peak	SJA	30
	7	4572.653	0.565	Kitt Peak	SJA	30
	8	4572.736	0.629	Kitt Peak	SJA	30
	9	4654.643	0.441	Kitt Peak	SJA/DMP	20
HD 34452[4]	13	4570.693	0.807	Kitt Peak	SJA	30
	14	4570.981	0.923	Kitt Peak	SJA	30
	15	4571.982	0.329	Kitt Peak	SJA	30
	16	4512.710	0.624	Kitt Peak	SJA	30
	17	4572.974	0.731	Kitt Peak	SJA	30
	18	4574.954	0.534	Kitt Peak	SJA	30
	19	4651.733	0.667	Kitt Peak	SJA/DMP	20
	20	4654.633	0.843	Kitt Peak	SJA/DMP	20
	21	4654.744	0.888	Kitt Peak	SJA/DMP	20
	22	4655.746	0.294	Kitt Peak	SJA/DMP	20
ε UMa	1	1355.059	0.603	Mt. Wilson	DMP	20
	2	1401.843	0.797	Kitt Peak	DMP	10
	3	1404.833	0.384	Kitt Peak	DMP	10
	4	1488.680	0.862	Mt. Wilson	DMP	20
	5	1492.687	0.649	Mt. Wilson	DMP	20
	6	1493.668	0.842	Mt. Wilson	DMP	20
	7	1794.839	0.026	Kitt Peak	DMP	10
	8	1795.839	0.223	Kitt Peak	DMP	10
	9	1796.829	0.417	Kitt Peak	DMP	10
	10	1847.697	0.413	Kitt Peak	DMP	10
	11	2143.845	0.611	Kitt Peak	DMP	20
	12	2144.838	0.806	Kitt Peak	DMP	20
	13	2145.806	0.996	Kitt Peak	DMP	20
	14	2202.758	0.188	Kitt Peak	DMP	20
	15	2203.663	0.366	Kitt Peak	DMP	20
	16	2206.653	0.953	Kitt Peak	DMP	20
	17	2207.733	0.166	Kitt Peak	DMP	20
	18	2208.654	0.347	Kitt Peak	DMP	20
	19	4569.042	0.195	Kitt Peak	SJA	4
	20	4571.049	0.590	Kitt Peak	SJA	4
	21	4572.050	0.786	Kitt peak	SJA	4
	22	4575.050	0.376	Kitt Peak	SJA	4
	23	4648.900	0.889	Kitt Peak	SJA/DMP	4
	24	4651.851	0.468	Kitt Peak	SJA/DMP	4
	25	4652.054	0.508	Kitt Peak	SJA/DMP	4
	26	4653.841	0.860	Kitt Peak	SJA/DMP	4
	27	4654.826	0.053	Kitt Peak	SJA/DMP	4
	28	4655.055	0.098	Kitt Peak	SJA/DMP	4
	29	4655.816	0.248	Kitt peak	SJA/DMP	4

TABLE II *(continued)*.

Star	Scan No.	JD(Hel.) 2440000+	Phase[1]	Observatory	Observer[2]	Bandpass[3] (Å)
CQ UMa	1	1795.872	0.863	Kitt Peak	DMP	20
	2	1796.871	0.271	Kitt Peak	DMP	20
	3	2142.878	0.500	Kitt Peak	DMP	20
	4	2143.914	0.923	Kitt Peak	DMP	20
	5	2144.819	0.292	Kitt Peak	DMP	20
	6	2145.838	0.708	Kitt Peak	DMP	20
	7	2202.786	0.953	Kitt Peak	DMP	20
	8	2203.759	0.350	Kitt Peak	DMP	20
	9	2205.740	0.159	Kitt Peak	DMP	20
	10	2207.758	0.982	Kitt Peak	DMP	20
	11	2208.737	0.382	Kitt Peak	DMP	20
	12	4648.994	0.419	Kitt Peak	SJA/DMP	20
	13	4651.864	0.590	Kitt Peak	SJA/DMP	20
	14	4651.956	0.628	Kitt Peak	SJA/DMP	20
	15	4652.040	0.662	Kitt Peak	SJA/DMP	20
	16	4653.896	0.420	Kitt Peak	SJA/DMP	20
	17	4654.866	0.816	Kitt Peak	SJA/DMP	20
	18	4654.945	0.848	Kitt Peak	SJA/DMP	20
	19	4655.006	0.873	Kitt Peak	SJA/DMP	20
	20	4655.860	0.221	Kitt Peak	SJA/DMP	20
	21	4655.929	0.250	Kitt Peak	SJA/DMP	20
	22	4655.992	0.275	Kitt Peak	SJA/DMP	20
CU Vir[5]	32	3583.917	0.943	Kitt Peak	SJA	30
	33	4648.974	0.467	Kitt Peak	SJA/DMP	20
	34	4649.011	0.539	Kitt Peak	SJA/DMP	20
	35	4651.921	0.128	Kitt Peak	SJA/DMP	20
	36	4651.941	0.165	Kitt Peak	SJA/DMP	20
	37	4651.972	0.226	Kitt Peak	SJA/DMP	20
	38	4651.989	0.258	Kitt Peak	SJA/DMP	20
	39	4652.019	0.315	Kitt Peak	SJA/DMP	20
	40	4653.908	0.944	Kitt Peak	SJA/DMP	20
	41	4653.933	0.991	Kitt Peak	SJA/DMP	20
	42	4653.949	0.022	Kitt Peak	SJA/DMP	20
	43	4654.891	0.832	Kitt Peak	SJA/DMP	20
	44	4654.910	0.867	Kitt Peak	SJA/DMP	20
	45	4654.932	0.911	Kitt Peak	SJA/DMP	20
	46	4655.025	0.089	Kitt Peak	SJA/DMP	20
	47	4655.871	0.714	Kitt peak	SJA/DMP	20
	48	4655.890	0.751	Kitt Peak	SJA/DMP	20
	49	4655.909	0.787	Kitt Peak	SJA/DMP	20
CS Vir	1	1401.902	0.226	Kitt Peak	DMP	20
	2	1404.901	0.549	Kitt Peak	DMP	20
	3	2111.949	0.613	Kitt Peak	DMP	20
	4	2142.909	0.944	Kitt Peak	DMP	20
	5	2143.914	0.052	Kitt Peak	DMP	20
	6	2144.890	0.157	Kitt Peak	DMP	20
	7	2202.735	0.380	Kitt Peak	DMP	20
	8	2203.717	0.486	Kitt Peak	DMP	20
	9	2207.705	0.915	Kitt Peak	DMP	20
	10	2208.697	0.021	Kitt Peak	DMP	20
	11	4649.036	0.553	Kitt Peak	SJA/DMP	20
	12	4652.004	0.873	Kitt Peak	SJA/DMP	20
	13	4654.989	0.194	Kitt Peak	SJA/DMP	20
	14	4655.977	0.300	Kitt Peak	SJA/DMP	20
β CrB	1	1401.954	0.622	Kitt Peak	DMP	20
	2	1404.942	0.784	Kitt Peak	DMP	20
	3	1416.926	0.432	Kitt Peak	DMP	20
	4	1417.947	0.487	Kitt Peak	DMP	20
	5	1492.775	0.535	Mt. Wilson	DMP	20
	6	1493.754	0.588	Mt. Wilson	DMP	20
	7	1757.032	0.829	Mt. Wilson	SJA	25
	8	1847.754	0.736	Kitt Peak	DMP	20
	9	2142.960	0.704	Kitt Peak	DMP	20
	10	2143.954	0.758	Kitt Peak	DMP	20
	11	2144.952	0.812	Kitt Peak	DMP	20
	12	2145.903	0.864	Kitt Peak	DMP	20
	13	2202.816	0.942	Kitt Peak	DMP	20
	14	2203.790	0.995	Kitt Peak	DMP	20
	15	2207.796	0.212	Kitt Peak	DMP	20
	16	2208.766	0.264	Kitt Peak	DMP	20
	17	2522.770	0.249	Kitt Peak	SJA	30
	18	2524.804	0.359	Kitt Peak	SJA	30
	19	2526.740	0.464	Kitt Peak	SJA	30
	20	2527.752	0.519	Kitt Peak	SJA	30
	21	2528.748	0.573	Kitt Peak	SJA	30
	22	2529.778	0.628	Kitt Peak	SJA	30
	23	2636.704	0.412	Palomar	SJA	25
	24	2637.701	0.466	Palomar	SJA	25
	25	2639.673	0.573	Palomar	SJA	25
	26	2640.669	0.627	Palomar	SJA	25
	27	2641.681	0.681	Palomar	SJA	25
	28	3232.913	0.662	Kitt Peak	SJA	30
	29	4654.965	0.584	Kitt Peak	SJA/DMP	20
	30	4655.917	0.636	Kitt Peak	SJA/DMP	20

Notes: [1]Calculated from ephmerides given in text.
[2]DMP = Pyper, SJA = Adelman.
[3]Second order is given. First order bandpasses are twice as large.
[4]Continuation of data from Paper VI.
[5]Continuation of data from Paper IV.

TABLE III. — *Comparison of Strömgren uvby photometry for Ap and comparison stars.*

Star	HD	V	u-b	b-y	m_1	n	References
63 And	14392	---	0.771	-0.060	0.160	1	Cameron (1966)
		---	0.883	-0.035	0.124	2+	Johansen and Gyldenkerne (1970)
		---	0.763	-0.037	0.133	3	Crawford, et al. (1972)
		---	0.768	-0.035	---	9	This paper (spectrophotometry)
HR 1732	34452	---	0.468	-0.130	0.185	1	Cameron (1966)
		---	0.405	-0.122	0.136	2+	Johansen and Gyldenkerne (1970)
		---	0.452	-0.126	0.178	5	Crawford, et al. (1972)
		---	0.437	-0.116	---	12	Paper VI
		---	0.439	-0.125	---	10	This paper (spectrophotometry)
		---	0.440	-0.125	---	22	New total (spectrophotometry)
		5.372	0.451	-0.122	0.153	21	This paper (photometry)
	(σ)	(0.008)	(0.007)	(0.006)	(0.015)		
HR 1752	34790	---	1.416	0.017	0.190	2	Johansen and Gyldenkerne (1970)
		---	1.441	0.019	0.194	3	Crawford, et al. (1972)
		5.658[2]	1.420	0.015	0.182	23	This paper (photometry)
	(σ)	(0.016)	(0.012)	(0.012)	(0.015)		
ε UMa	112185	---	1.468	-0.015	0.184	3	Crawford and Barnes (1969)
		---	1.455	-0.014	0.168	5	Cameron (1966)
		---	1.409	-0.015	0.140	2+	Johansen and Gyldenkerne (1970)
		---	1.472	-0.014	0.168	7	Crawford, et al. (1972)
		---	1.451	-0.024	---	29	This paper (spectrophotometry)
		1.762	1.443	-0.012	0.156	20	This paper (photometry)
	(σ)	(0.007)	(0.010)	(0.005)	(0.013)		
δ UMa	106591	---	1.499	0.040	0.183	3	Crawford, et al. (1966)
		---	1.501	0.040	0.183	5	Crawford and Barnes (1969)
		---	1.499	0.042	0.179	6	Perry (1969)
		3.313	1.498[3]	0.043	0.171	20	This paper (photometry)
	(σ)	(0.008)	(0.016)	(0.006)	(0.009)		
CQ UMa	119213	6.27	1.406	0.043	0.242	25	Wolff and Morrison (1975)
		---	1.376	0.033	---	22	This paper (spectrophotometry)
		6.284	1.385	0.040	0.235[4]	25	This paper (photometry)
	(σ)	(0.004)	(0.006)	(0.015)	(0.010)		
HR 5216	120874	---	1.468	0.036	0.210	7	Crawford, et al. (1972)
		6.453	1.457	0.046	0.175	25	This paper (photometry)
	(σ)	(0.014)	(0.014)	(0.010)	(0.011)		
CU Vir[1]	124224	---	0.730	-0.061	---	32	Paper IV (spectrophotometry)
		---	0.725	-0.065	---	18	This paper (spectrophotometry)
		---	0.727	-0.065	---	49	New total (spectrophotometry)
		5.006	0.724	-0.060	0.133[5]	23	This paper (photometry)
	(σ)	(0.023)	(0.029)	(0.009)	(0.013)		
τ Vir	122408	---	1.569	0.062	0.164	2	Crawford, et al. (1966)
		4.258	1.605	0.064	0.157	22	This paper (photometry)
	(σ)	(0.012)	(0.014)	(0.007)	(0.011)		
CS Vir	125248	---	1.305	-0.038	0.206	4	Cameron (1966)
		5.90	1.286	-0.026	0.247	13	Wolff and Wolff (1971)
		---	1.239	-0.058	---	2	Stokes (1972)
		5.73	1.248	-0.045	0.231	5	Warren (1973)
		---	1.297	-0.058	---	2	Gronbech and Olsen (1976)
		---	1.283	-0.038	---	14	This paper (spectrophotometry)
		5.910	1.293	-0.039	0.230[6]	12	This paper (photometry)
	(σ)	(0.019)	(0.023)	(0.027)	(0.016)		
HR 5335	124683	---	1.269	0.004	0.141	13	Wolff and Wolff (1971)
		---	1.268	-0.019	0.153	2	Stokes (1972)
		5.580	1.276	-0.004	0.141	12	This paper (photometry)
	(σ)	(0.023)	(0.018)	(0.009)	(0.007)		
β CrB	137909	---	1.530	0.140	---	3	Crawford, et al. (1966)
		---	1.557	0.145	---	3	Cameron (1966)
		3.65	1.538	0.150	0.250	25	Wolff and Wolff (1971)
		---	1.544	0.138	---	30	This paper (spectrophotometry)
		3.666	1.559	0.148	0.236	14	This paper (photometry)
	(σ)	(0.008)	(0.009)	(0.006)	(0.017)		
γ CrB	140436	3.816	1.335	0.009	0.147	14	This paper (photometry)
	(σ)	(0.016)	(0.013)	(0.006)	(0.006)		

Notes: [1]See Paper IV for other four-color references.
[2]n = 21
[3]n = 19
[4]n = 8
[5]n = 22
[6]n = 5

TABLE IV. — *Four-color and Hβ photometry.*

Star	JD(Hel.) 2440000+	Phase	b-y	u-b	y	b	v	u	β
HD 34452	4217.845	0.733	-0.119	0.456	5.335	5.195	5.237	5.672	2.697
	4221.922	0.386	-0.119	0.446	5.335	5.194	5.231	5.664	2.697
	4222.801	0.743	-0.115	0.459	5.328	5.197	5.247	5.672	2.707
	4588.922	0.198	-0.122	0.451	5.318	5.184	5.218	5.646	2.697
	4590.861	0.984	-0.118	0.460	5.342	5.202	5.246	5.665	2.700
	4928.955	0.076	-0.123	0.454	5.324	5.199	5.234	5.651	2.696
	4931.952	0.291	-0.122	0.454	5.320	5.197	5.238	5.652	2.698
	4932.923	0.684	-0.111	0.445	5.332	5.207	5.248	5.660	2.696
	4933.918	0.088	-0.121	0.447	5.328	5.207	5.229	5.654	2.703
	4934.808	0.449	-0.124	0.446	5.338	5.208	5.246	5.660	2.702
	5441.618	0.951	-0.128	0.453	5.332	5.201	5.245	5.657	---
	5442.619	0.357	-0.126	0.464	5.329	5.198	5.231	5.660	---
	5443.621	0.763	-0.119	0.447	5.328	5.202	5.249	5.673	---
	5444.614	0.166	-0.134	0.463:	5.318	5.184	5.219	5.647	---
	5620.908	0.650	-0.111	0.439	5.333	5.212	5.255	5.659	2.684
	5622.882	0.450	-0.125	0.445	5.330	5.195	5.240	5.672	2.673
	5627.904	0.487	-0.130	0.445	5.339	5.210	5.227	5.665	2.682
	5782.678	0.245	-0.128	0.457	5.321	5.193	5.220	5.650	---
	5783.652	0.640	-0.115	0.442	5.338	5.218	5.256	5.660	---
	5785.649	0.450	-0.127	0.448	5.323	5.196	5.234	5.666	2.703
	5787.653	0.262	-0.120	0.451	5.312	5.192	5.218	5.643	---
ε UMa	4338.850	0.960	-0.019	1.428	1.710	1.691	1.835	3.119	2.859
	4339.776	0.141	-0.008	1.439	1.720	1.712	1.849	3.151	2.875
	4340.758	0.334	-0.008	1.448	1.732	1.722	1.864	3.172	2.883
	4341.780	0.535	-0.013	1.446	1.725	1.712	1.858	3.158	2.879
	4342.761	0.728	-0.016	1.449	1.732	1.716	1.850	3.165	2.871
	4343.750	0.922	-0.014	1.428	1.710	1.696	1.852	3.124	2.856
	4742.753	0.332	-0.004	1.445	1.721	1.717	1.867	3.162	2.860
	4743.640	0.506	-0.015	1.456	1.724	1.709	1.862	3.165	2.884
	4745.640	0.899	-0.016	1.431	1.711	1.695	1.850	3.126	2.861
	4746.644	0.097	-0.009	1.444	1.715	1.706	1.853	3.150	2.854
	4746.722	0.112	-0.014	1.428	1.718	1.704	1.847	3.132	2.847
	5440.747	0.498	-0.006	1.444	1.720	1.714	1.861	3.158	2.864
	5441.765	0.698	-0.009	1.451	1.728	1.719	1.857	3.170	2.865
	5442.752	0.892	-0.018	1.437	1.716	1.698	1.842	3.135	2.854
	5443.754	0.088	-0.016	1.433	1.718	1.702	1.848	3.135	2.866
	5444.749	0.284	-0.008	1.437	1.731	1.722	1.853	3.159	2.858
	5782.814	0.718	-0.012	1.463	1.722	1.713	1.860	3.169	2.866
	5783.746	0.901	-0.020	1.445	1.713	1.705	1.851	3.151	1.867
	5785.737	0.293	-0.015	1.453	1.727	1.716	1.862	2.168	2.860
	5787.727	0.684	-0.006	1.451	1.731	1.714	1.862	3.165	2.897
CQ UMa	4338.877	0.837	0.032	1.389	6.247	6.279	6.535	7.667	2.912
	4339.840	0.230	0.031	1.396	6.234	6.289	6.555	7.686	---
	4340.850	0.642	0.048	1.385	6.245	6.293	6.565	7.678	2.899
	4341.909	0.075	0.024	1.388	6.245	6.269	6.525	7.657	2.877
	4342.826	0.449	0.066	1.385	6.238	6.305	6.603	7.676	2.855
	4343.778	0.839	0.022	1.388	6.251	6.274	6.533	7.662	2.894
	4742.809	0.709	0.019	1.382	6.243	6.279	6.544	7.676	2.883
	4743.708	0.076	0.028	1.384	6.243	6.271	6.508	7.654	2.882
	4745.707	0.892	0.011	1.394	6.247	6.258	6.513	7.652	2.882
	4746.699	0.297	0.053	1.384	6.249	6.302	6.596	7.686	2.855
	5440.816	0.614	0.046	1.391	6.242	6.289	6.574	7.680	2.890
	5441.808	0.019	0.020	1.390	6.239	6.258	6.520	7.648	2.894
	5442.807	0.426	0.059	1.383	6.246	6.305	6.614	7.687	2.868
	5443.792	0.828	0.032	1.382	6.244	6.276	6.529	7.657	2.898
	5444.813	0.245	0.042	1.389	6.246	6.289	6.575	7.678	2.885
	5471.777	0.250	0.051	1.386	6.245	6.296	6.578	7.682	2.862
	5472.814	0.674	0.051	1.386	6.247	6.286	6.575	7.685	2.898
	5474.714	0.450	0.055	1.372	6.239	6.303	6.600	7.666	2.867
	5475.715	0.858	0.029	1.384	6.245	6.273	6.531	7.657	2.914
	5476.704	0.262	0.050	1.386	6.243	6.293	6.583	7.679	2.886
	5477.699	0.668	0.036	1.392	6.251	6.287	6.559	7.679	2.893
	5782.861	0.266	0.042	1.380	6.249	6.290	6.555	7.670	2.904
	5783.833	0.622	0.046	1.374	6.246	6.292	6.557	7.687	2.907
	5785.819	0.433	0.059	1.373	6.249	6.309	6.605	7.681	2.888
	5787.812	0.247	0.055	1.377	6.242	6.298	6.573	7.675	2.897

TABLE IV *(continued)*.

Star	JD(Hel.) 2440000+	Phase	b-y	u-b	y	b	v	u	β
CU Vir	4338.898	0.943	-0.052	0.751	5.004	4.952	5.035	5.706	2.761
	4339.861	0.792	-0.059	0.717	4.978	4.919	5.010	5.636	2.749
	4340.882	0.753	-0.061	0.707	4.960	4.910	4.974	5.628	2.751
	4341.896	0.700	-0.057	0.685	4.951	4.894	4.958	5.592	2.750
	4342.846	0.525	-0.064	0.673	4.931	4.866	---	5.547	2.737
	4742.780	0.630	-0.060	0.684	4.939	4.879	4.948	5.553	2.733
	4743.670	0.338	-0.074	0.724	4.943	4.869	4.948	5.583	2.755
	4743.741	0.474	-0.056	0.685	4.941	4.885	4.942	5.558	2.740
	4745.670	0.179	-0.065	0.746	4.982	4.916	4.982	5.645	2.777
	4745.729	0.292	-0.073	0.725	4.956	4.882	4.941	5.603	2.759
	4746.644	0.097	-0.064	0.758	5.000	4.936	5.012	5.705	2.752
	4746.741	0.237	-0.066	0.746	4.962	4.896	4.953	5.650	2.767
	5441.823	0.195	-0.073	0.737	4.959	4.887	4.965	5.646	2.753
	5443.803	0.997	-0.045	0.750	4.994	4.941	5.016	5.710	2.759
	5444.835	0.981	-0.057	0.759	4.991	4.942	5.024	5.700	2.757
	5471.821	0.808	-0.052	0.708	4.985	4.933	5.007	5.641	2.732
	5472.730	0.544	-0.059	0.678	4.941	4.882	4.949	5.552	2.737
	5472.837	0.761	-0.044	0.686	4.964	4.895	4.968	5.596	2.763
	5474.734	0.403	-0.061	0.753	4.940	4.879	4.950	5.598	2.755
	5475.732	0.319	-0.069	0.748	4.940	4.870	4.940	5.615	2.776
	5476.725	0.226	-0.071	0.753	4.965	4.904	4.976	5.657	2.785
	5476.795	0.362	-0.062	0.729	4.935	4.873	4.938	5.602	2.775
	5477.716	0.130	-0.047	0.743	4.982	4.936	5.001	5.686	2.776
CS Vir	5440.834	0.735	-0.046	1.287	5.879	5.833	5.995	7.120	2.872
	5441.839	0.843	-0.020	1.327	5.869	5.838	6.027	7.166	2.873
	5443.820	0.056	0.002	1.322	5.833	5.845	6.097	7.166	2.853
	5444.823	0.164	-0.015	1.315	5.856	5.841	6.061	7.155	2.873
	5472.767	0.705	-0.019	1.310	5.855	5.847	6.070	7.155	2.874
	5474.753	0.598	-0.054	1.280	5.893	5.839	6.015	7.119	2.857
	5475.749	0.491	-0.061	1.274	5.881	5.820	5.978	7.095	2.872
	5476.743	0.598	-0.067	1.261	5.864	5.829	5.966	7.090	2.856
	5477.734	0.705	-0.055	1.295	5.877	5.822	6.010	7.117	2.885
	5782.906	0.535	-0.072	1.270	5.887	5.809	5.959	7.079	2.885
	5783.899	0.642	-0.064	1.265	5.882	5.818	5.971	7.083	2.905
	5787.881	0.070	0.003	1.306	5.839	5.841	6.086	7.147	2.853
β CrB	5440.908	0.097	0.143	1.568	3.631	3.774	4.148	5.328	2.858
	5441.884	0.150	0.148	1.566	3.626	3.774	4.128	5.339	2.842
	5443.862	0.257	0.152	1.569	3.615	3.768	4.144	5.337	2.849
	5444.880	0.312	0.145	1.568	3.625	6.769	4.135	5.345	2.849
	5471.895	0.773	0.151	1.560	3.639	3.793	4.185	5.347	2.834
	5472.863	0.826	0.153	1.560	3.637	3.790	4.186	5.349	2.844
	5474.774	0.929	0.152	1.549	3.634	3.787	4.176	5.339	2.828
	5475.768	0.983	0.156	1.540	3.639	3.781	4.182	5.335	2.852
	5476.767	0.037	0.149	1.557	3.628	3.777	4.164	5.333	2.850
	5477.755	0.090	0.142	1.564	3.626	3.767	4.150	5.331	2.849
	5782.956	0.599	0.146	1.555	3.364	3.779	4.173	5.335	---
	5783.935	0.652	0.133	1.567	3.624	3.788	4.156	5.324	2.857
	5785.907	0.759	0.147	1.548	3.644	3.791	4.181	5.338	2.900
	5787.859	0.865	0.150	1.550	3.641	3.791	4.194	5.342	2.846

TABLE V. — *Temperature estimates.*

Star	Spectrophotometric Fitting PC[1]	BJ[3]	u-b[5]	Literature[7]	References
63 And	10750 K	12900 K	12800 K	13250 K	Mihalas and Henshaw (1966)
				13625 K	Megessier (1971)
HD 34452	15800 K	15800 K	15800 K	15750 K	Paper VI[9]
ε UMa	9500 K[2]	9000 K[2]	9120 K[2]	9300 K[8]	Engin (1976)
				9500 K[6]	Mallama and Molnar (1977)
				8920 K[8]	Shallis and Blackwell (1979)
				9985 K[6]	Tektunali (1981)
CQ UMa	8650 K	10250 K	9570 K	8150 K	Glagolevskij, et al. (1981)
CU Vir	13000 K	13000 K	13100 K	13000 K	Paper IV[9]
CS Vir	9675 K	10375 K	10100 K	---	
β CrB	8000 K	8000 K[4]	8900 K[6]	8750 K	Hardorp and Shore (1971)
				9700 K	Adelman (1973)

Notes: [1]Red end of Paschen continuum matched to model.
[2]Globally, the best fit is to either a 9400 K, log g = 3.5 model or a 9500 K, log g = 3.0 model.
[3]Blue end of Paschen continuum (model) matched to λλ4032-4255.
[4]Balmer jump (but not Balmer continuum) also fit by 10000 K model.
[5]Synthesized u-b values compared to those of Relyea and Kurucz (1978).
[6]log g = 3.5.
[7]Log g = 4.0 unless otherwise noted.
[8]log g = 3.2.
[9]Contains references to earlier work.

TABLE VI. — *Continuous energy distributions (− 2.5 log F_ν/F_{5000}) for 63 And.*

λ(Å)	1	2	3	4	5	6	7	8	9[2]	Average
3300	0.554	0.551	0.546	0.542	0.529	0.539	0.545	0.548	0.551	0.545
3390	0.550	0.547	0.544	0.546	0.534	0.546	0.548	0.553	0.564	0.548
3448	0.549	0.543	0.550	0.550	0.542	0.546	0.542	0.558	0.568	0.550
3509	0.551	0.541	0.538	0.540	0.536	0.540	0.542	0.550	0.550	0.543
3540	0.543	0.538	0.538	0.530	0.525	0.536	0.533	0.542	0.562	0.539
3571	0.552	0.545	0.544	0.545	0.543	0.550	0.550	0.551	0.564	0.549
3636	0.545	0.541	0.542	0.535	0.533	0.541	0.545	0.541	0.554	0.542
3704	0.529	0.523	0.522	0.520	0.513	0.518	0.525	0.522	0.545	0.524
4032	-0.238	-0.249	-0.252	-0.253	-0.258	-0.252	-0.248	-0.236	-0.252	-0.249
4167	-0.204	-0.214	-0.206	-0.212	-0.209	-0.204	-0.199	-0.191	-0.202	-0.205
4200	-0.193	-0.194	-0.190	-0.192	-0.193	-0.182	-0.180	-0.181	-0.189	-0.188
4255	-0.178	-0.183	-0.190	-0.191	-0.195	-0.185	-0.190	-0.177	-0.186	-0.186
4340	0.299	0.227	0.205	0.211	0.202	0.220	0.207	0.215	0.347	0.229
4464	-0.156	-0.159	-0.166	-0.172	-0.176	-0.160	-0.160	-0.155	-0.161	-0.163
4566	-0.128	-0.124	-0.127	-0.125	-0.140	-0.118	-0.112	-0.113	-0.122	-0.123
4673	-0.098	-0.087	-0.092	-0.089	-0.108	-0.084	-0.091	-0.090	-0.097	-0.093
4785	-0.070	-0.064	-0.063	-0.070	-0.071	-0.065	-0.072	-0.058	-0.062	-0.066
4861	0.320	0.313	0.306	0.312	0.315	0.308	0.311	0.309	0.393	0.321
4935	-0.029	-0.029	-0.018	-0.033	-0.033	-0.019	-0.030	-0.029	-0.021	-0.027
4975	-0.027	-0.020	-0.016	-0.025	-0.023	-0.015	-0.013	-0.015	-0.021	-0.019
5000	0.000	0.000	0.000	0.000	0.000	0.000	0.000	0.000	0.000	0.000
5060	0.018	0.018	0.026	0.018	0.021	0.021	0.027	0.030	0.028	0.023
5128	0.021	0.030	0.031	0.031	0.032	0.038	0.033	0.042	0.045	0.034
5200	0.061	0.055	0.062	0.072	0.065	0.065	0.068	0.069	0.070	0.065
5232	0.053	0.067	0.070	0.065	0.067	0.074	0.072	0.076	0.087	0.070
5264	0.054	0.057	0.064	0.060	0.062	0.071	0.068	0.071	0.072	0.064
5360	0.070	0.074	0.083	0.078	0.082	0.082	0.080	0.084	0.080	0.079
5470	0.093	0.095	0.100	0.100	0.093	0.100	0.098	0.100	0.119	0.100
5556	0.101	0.108	0.112	0.113	0.109	0.113	0.119	0.122	0.114	0.112
5700	0.136	0.140	0.133	0.129	0.143	0.152	0.133	0.139	0.150	0.139
5800	0.173	0.188	0.171	0.180	0.182	0.196	0.185	0.188	0.193	0.184
5840	0.168	0.174	0.166	0.168	0.168	0.179	0.160	0.176	0.176	0.171
5875	0.185	0.197	0.189	0.192	0.191	0.189	0.202	0.199	0.204	0.194
6020	0.203	0.210	0.210	0.211	0.201	0.214	0.215	0.211	0.225	0.211
6058	0.214	0.217	0.222	0.212	0.217	0.229	0.225	0.220	0.225	0.220
6220	0.247	0.246	0.267	0.250	0.249	0.258	0.263	0.264	0.279	0.258
6300	0.252	0.261	0.272	0.267	0.267	0.283	0.271	0.276	0.296	0.272
6370	0.274	0.279	0.285	0.290	0.285	0.294	0.289	0.299	0.328	0.291
6440	0.279	0.297	0.304	0.307	0.310	0.308	0.305	0.312	0.319	0.305
6563	0.458	0.471	0.474	0.471	0.465	0.480	0.468	0.474	0.567	0.481
6650	0.315	0.330	0.346	0.339	0.338	0.341	0.338	0.336	0.347	0.337
6710	0.327	0.327	0.338	0.338	0.341	0.333	0.340	0.345	0.362	0.339
6792	0.334	0.349	0.352	0.353	0.359	0.362	0.360	0.367	0.382	0.358
7102	0.392	0.412	0.397	0.405	0.406	0.412	0.410	0.409	0.423	0.407
u-b[1]	0.777	0.764	0.766	0.765	0.770	0.759	0.764	0.766	0.782	0.768
b-y[1]	-0.030	-0.027	-0.036	-0.034	-0.046	-0.032	-0.034	-0.034	-0.045	-0.035
Δa[1]	0.009	0.009	0.010	0.014	0.015	0.014	0.014	0.015	0.016	0.013
Δa'	0.004	0.000	0.011	0.010	0.014	0.013	0.023	0.011	0.016	0.011
Δι	0.003	0.005	0.017	0.014	0.020	0.019	0.023	0.014	0.018	0.015
Δι*	0.011	0.012	0.025	0.025	0.034	0.026	0.029	0.024	0.029	0.024
Δι**	0.011	0.009	0.018	0.017	0.023	0.018	0.016	0.017	0.020	0.017

Notes: (1) Balmer line bandpasses were not used in the calculation of u-b, b-y and Δa.
(2) Additional values: λ7530, m=0.509; λ7850, m=0.586.

TABLE VII. — *Continuous energy distributions ($-2.5 \log F_\nu/F_{5000}$) for HD 34452.*

λ(Å)	13	14	15	16	17	18
3300	0.160	0.182	0.133	0.162	0.143	0.154
3360	0.176	0.182	0.156	0.182	0.171	0.168
3390	0.190	0.191	0.171	0.185	0.174	0.178
3420	0.179	0.187	0.164	0.176	0.169	0.179
3448	0.198	0.198	0.168	0.198	0.173	0.185
3478	0.188	0.174	0.174	0.181	0.169	0.184
3509	0.169	0.180	0.174	0.185	0.174	0.183
3540	0.183	0.169	0.171	0.176	0.163	0.174
3571	0.174	0.194	0.182	0.190	0.179	0.182
3636	0.198	0.193	0.185	0.190	0.175	0.182
3704	0.189	0.197	0.163	0.184	0.169	0.176
4032	-0.333	-0.337	-0.351	-0.331	-0.340	-0.341
4055	-0.334	-0.324	-0.385	-0.338	-0.335	-0.333
4167	-0.269	-0.267	-0.266	-0.260	-0.261	-0.257
4200	-0.235	-0.228	-0.227	-0.228	-0.237	-0.236
4255	-0.246	-0.234	-0.254	-0.231	-0.234	-0.249
4340	0.062	0.079	0.055	0.069	0.068	0.049
4412	-0.199	-0.194	-0.222	-0.198	-0.200	-0.210
4464	-0.216	-0.201	-0.225	-0.202	-0.207	-0.215
4566	-0.165	-0.156	-0.173	-0.154	-0.158	-0.167
4673	-0.133	-0.130	-0.151	-0.139	-0.139	-0.143
4785	-0.094	-0.085	-0.094	-0.090	-0.093	-0.085
4861	0.204	0.221	0.202	0.206	0.211	0.206
4935	-0.056	-0.048	-0.059	-0.054	-0.049	-0.049
4975	-0.038	-0.036	-0.049	-0.043	-0.039	-0.038
5000	0.000	0.000	0.000	0.000	0.000	0.000
5060	0.029	0.041	0.045	0.025	0.042	0.023
5128	0.093	0.103	0.073	0.077	0.092	0.073
5200	0.163	0.164	0.160	0.150	0.166	0.148
5264	0.119	0.122	0.115	0.118	0.125	0.110
5360	0.134	0.146	0.135	0.124	0.137	0.121
5470	0.156	0.153	0.144	0.143	0.150	0.143
5556	0.152	0.173	0.142	0.149	0.159	0.144
5700	0.164	0.178	0.167	0.165	0.183	0.162
5800	0.226	0.242	0.222	0.227	0.240	0.220
5840	0.213	0.219	0.195	0.207	0.219	0.196
5875	0.231	0.244	0.224	0.226	0.238	0.227
6020	0.254	0.265	0.237	0.257	0.264	0.249
6058	0.262	0.280	0.263	0.258	0.279	0.262
6220	0.315	0.316	0.315	0.298	0.314	0.295
6370	0.366	0.370	0.369	0.368	0.372	0.368
6440	0.402	0.409	0.392	0.388	0.402	0.389
6563	0.513	0.529	0.511	0.508	0.525	0.516
6650	0.411	0.414	0.405	0.400	0.412	0.405
6710	0.421	0.421	0.408	0.406	0.413	0.410
6792	0.440	0.455	0.430	0.433	0.459	0.432
7102	0.504	0.516	0.491	0.497	0.514	0.498
u-b	0.440	0.440	0.436	0.439	0.427	0.439
b-y	-0.126	-0.128	-0.131	-0.117	-0.129	-0.119
Δa	0.063	0.060	0.061	0.060	0.064	0.056
Δa'	0.074	0.069	0.078	0.072	0.077	0.066
Δι	0.038	0.039	0.057	0.037	0.039	0.048
Δι*	0.072	0.072	0.093	0.068	0.075	0.078
hb	0.279	0.288	0.279	0.278	0.282	0.273

λ(Å)	19	20	21	22	Avg. (13-22)	Avg.[1] (1-22)
3300	0.162	0.162	0.170	0.150	0.158	0.161
3360	0.185	0.177	0.190	0.172	0.176	0.177
3390	0.198	0.190	0.199	0.190	0.187	0.187
3420	0.182	0.179	0.189	0.171	0.178	0.178
3448	0.190	0.186	0.208	0.183	0.189	0.189
3478	0.187	0.178	0.193	0.182	0.181	0.182
3509	0.176	0.193	0.205	0.174	0.181	0.182
3540	0.177	0.181	0.181	0.201	0.178	0.178
3571	0.198	0.181	0.202	0.188	0.187	0.187
3636	0.192	0.192	0.219	0.184	0.191	0.190
3704	0.203	0.195	0.211	0.190	0.188	0.191
4032	-0.325	-0.335	-0.327	-0.311	-0.333	-0.327
4055	-0.329	-0.323	-0.324	-0.332	-0.331	-0.327
4167	-0.268	-0.275	-0.258	-0.276	-0.266	-0.263
4200	-0.228	-0.224	-0.198	-0.217	-0.226	-0.225
4255	-0.244	-0.240	-0.224	-0.239	-0.240	-0.237
4340	0.183	0.187	0.186	0.178	---	---
4412	-0.187	-0.182	-0.173	-0.187	-0.195	-0.192
4464	-0.224	-0.207	-0.199	-0.215	-0.211	-0.208
4566	-0.170	-0.168	-0.162	-0.161	-0.163	-0.159
4673	-0.137	-0.136	-0.118	-0.132	-0.136	-0.133
4785	-0.093	-0.096	-0.077	-0.099	-0.091	-0.090
4861	0.304	0.302	0.290	0.315	---	---
4935	-0.041	-0.041	-0.025	-0.046	-0.047	-0.046
4975	-0.038	-0.043	-0.031	-0.036	-0.039	-0.038
5000	0.000	0.000	0.000	0.000	0.000	0.000
5060	0.043	0.038	0.057	0.038	0.038	0.038
5128	0.106	0.091	0.099	0.079	0.089	0.087
5200	0.168	0.176	0.189	0.157	0.164	0.163
5264	0.121	0.124	0.136	0.108	0.120	0.119
5360	0.130	0.130	0.155	0.126	0.134	0.135
5470	0.156	0.155	0.167	0.154	0.152	0.153
5556	0.141	0.143	0.166	0.150	0.152	0.150
5700	0.170	0.186	0.200	0.174	0.175	0.172
5800	0.229	0.245	0.260	0.244	0.236	0.232
5840	0.201	0.219	0.225	0.202	0.210	0.206
5875	0.239	0.241	0.262	0.250	0.238	0.233
6020	0.252	0.247	0.273	0.263	0.256	0.252
6058	0.275	0.262	0.284	0.265	0.269	0.262
6220	0.295	0.302	0.321	0.308	0.308	0.302
6370	0.360	0.366	0.402	0.370	0.371	0.362
6440	0.404	0.408	0.421	0.409	0.402	0.392
6563	0.579	0.582	0.601	0.575	---	---
6650	0.394	0.405	0.442	0.421	0.411	0.401
6710	0.415	0.418	0.442	0.417	0.417	0.406
6792	0.439	0.443	0.459	0.449	0.444	0.432
7102	0.497	0.492	0.529	0.507	0.504	0.491
7530	0.605	0.618	0.628	0.602	0.613	0.594
7850	0.657	0.650	0.662	0.670	0.660	0.646
u-b	0.447	0.443	0.441	0.436	0.439	0.440
b-y	-0.132	-0.127	-0.130	-0.121	-0.125	-0.125
Δa	0.062	0.068	0.067	0.054	0.063	0.061
Δa'	0.081	0.077	0.076	0.070	0.074	0.074
Δι	0.038	0.039	0.048	0.029	0.039	0.038
Δι*	0.079	0.071	0.086	0.064	0.075	0.073
hb	0.371	0.371	0.341	0.388	---	---

Note: [1]) Does not include R.E.W. ultraviolet values.
Additional value: λ4722: m = 0.128

TABLE VIII. — *Continuous energy distributions (− 2.5 log F_ν/F_{5000}) for ε UMa.*

λ(Å)	1	2	3	4	5	6	7	8	9
3390	---	1.282	1.285	---	---	---	1.283	1.295	1.281
3448	---	1.253	1.253	---	---	---	1.244	1.281	1.274
3509	---	1.226	1.236	---	---	---	1.215	1.248	1.211
3571	---	1.195	1.218	---	---	---	1.211	1.231	1.220
3636	---	1.172	1.190	---	---	---	1.177	1.194	1.183
4032	-0.225	-0.215	-0.182	-0.180	-0.179	-0.186	-0.189	-0.208	-0.187
4167	-0.188	-0.150	-0.163	-0.171	-0.176	-0.169	-0.172	-0.175	-0.156
4255	-0.150	-0.151	-0.141	-0.160	-0.162	-0.161	-0.136	-0.136	-0.164
4464	-0.152	-0.141	-0.126	-0.175	-0.163	-0.170	-0.117	-0.115	---
4566	-0.117	-0.138	-0.112	-0.118	-0.112	-0.119	-0.111	-0.098	-0.101
4785	-0.068	-0.076	-0.051	-0.073	-0.065	-0.075	-0.072	-0.052	-0.061
5000	0.000	0.000	0.000	0.000	0.000	0.000	0.000	0.000	0.000
5263	0.069	0.065	0.060	0.071	0.064	0.066	0.092	0.087	0.071
5556	0.116	0.103	0.097	0.107	0.105	0.096	0.121	0.115	0.105
5840	0.165	0.120	0.123	0.144	0.154	0.145	0.176	0.155	0.148
6055	0.211	0.191	0.206	0.194	0.203	0.192	0.195	0.212	0.207
6370	0.260	0.248	0.253	0.254	0.256	0.247	0.251	0.265	0.256
6800	0.318	0.311	0.297	0.300	0.307	0.289	0.322	0.315	0.317
7100	0.345	0.356	0.338	---	0.356	0.341	0.374	0.375	0.371
7530	0.450	0.425	0.401	0.456	0.464	0.436	0.462	0.475	0.461
7850	0.498	0.493	0.442	0.494	0.508	0.468	0.497	0.502	0.490
u-b	---	1.481	1.467	---	---	---	1.467	1.465	1.456
b-y	-0.039	-0.043	-0.012	-0.039	-0.027	-0.031	-0.049	-0.027	-0.023
Δa	0.009	0.011	0.007	0.013	0.008	0.012	0.021	0.018	0.012
Δa'	0.026	0.047	0.021	0.040	0.022	0.034	0.048	0.037	0.029

λ(Å)	10	11	12	13	14	15	16	17	18
3390	1.297	1.307	1.294	1.284	1.300	1.271	1.286	1.283	1.332
3448	1.277	1.277	1.251	1.254	1.271	1.254	1.260	1.251	1.285
3509	1.227	1.248	1.230	1.223	1.244	1.238	1.220	1.202	1.260
3571	1.225	1.214	1.215	1.206	1.237	1.205	1.216	1.192	1.232
3636	1.179	1.181	1.179	1.167	1.204	1.176	1.178	1.170	1.205
4032	-0.174	-0.203	-0.203	-0.203	-0.176	-0.184	-0.232	-0.213	-0.154
4167	-0.185	-0.171	-0.166	-0.157	-0.157	-0.163	-0.146	-0.184	-0.132
4255	-0.148	-0.147	-0.148	-0.142	-0.124	-0.151	-0.122	-0.146	-0.128
4464	-0.112	-0.132	-0.138	-0.139	-0.090	-0.139	-0.169	-0.143	-0.109
4566	-0.101	-0.109	-0.106	-0.103	-0.051	-0.079	-0.092	-0.081	-0.082
4785	-0.062	-0.074	-0.074	-0.080	-0.037	-0.063	-0.057	-0.061	-0.071
5000	0.000	0.000	0.000	0.000	0.000	0.000	0.000	0.000	0.000
5263	0.078	0.068	0.079	0.072	0.080	0.055	0.099	0.064	0.058
5556	0.105	0.103	0.101	0.097	0.135	0.100	0.115	0.117	0.114
5840	0.151	0.157	0.149	0.141	0.192	0.159	0.147	0.175	0.157
6055	0.181	0.207	0.198	0.184	0.218	0.196	0.196	0.207	0.207
6370	0.253	0.260	0.262	0.239	0.282	0.238	0.251	0.259	0.261
6800	0.322	0.333	0.326	0.318	0.338	0.301	0.320	0.323	0.313
7100	0.358	0.374	0.376	0.364	0.384	0.350	0.369	0.374	0.373
7530	0.437	0.468	0.468	0.454	0.469	0.439	0.456	0.453	0.454
7850	0.518	0.519	0.512	0.499	0.503	0.481	0.501	0.519	0.501
u-b	1.466	1.485	1.476	1.466	1.441	1.442	1.453	1.442	1.494
b-y	-0.023	-0.028	-0.030	-0.026	-0.004	-0.001	-0.031	-0.014	-0.012
Δa	0.016	0.011	0.018	0.015	0.007	0.003	0.025	0.004	0.003
Δa'	0.035	0.029	0.044	0.044	0.002	0.005	0.056	0.008	0.015

TABLE VIII *(continued)*.

λ(Å)	19	20	21	22	23	24	25	26	27	28	29	Average
3300	1.289	1.289	1.268	1.271	1.262	1.274	1.277	1.268	1.237	1.259	1.270	1.273
3390	1.304	1.306	1.295	1.292	1.257	1.300	1.297	1.300	1.267	1.252	1.299	1.290
3448	1.285	1.244	1.230	1.263	1.199	1.225	1.215	1.214	1.210	1.213	1.231	1.249
3509	1.250	1.248	1.244	1.226	1.182	1.221	1.230	1.220	1.195	1.211	1.233	1.228
3540	1.230	1.204	1.193	1.210	1.151	1.187	1.182	1.185	1.174	1.184	1.198	1.198
3571	1.253	1.232	1.218	1.229	1.178	1.204	1.203	1.195	1.203	1.216	1.226	1.215
3636	1.200	1.174	1.162	1.176	1.138	1.157	1.156	1.156	1.155	1.148	1.172	1.174
3704	1.170	1.169	1.124	1.166	0.926	1.004	1.016	1.126	1.164	1.176	1.141	1.116
4032	-0.178	-0.200	-0.222	-0.197	-0.248	-0.239	-0.241	-0.227	-0.192	-0.198	-0.202	-0.201
4167	-0.175	-0.189	-0.192	-0.177	-0.139	-0.207	-0.211	-0.197	-0.201	-0.201	-0.190	-0.174
4200	-0.108	-0.146	-0.132	-0.135	-0.171	-0.172	-0.171	-0.132	-0.121	-0.134	-0.143	-0.132
4255	-0.103	-0.161	-0.155	-0.133	-0.161	-0.166	-0.180	-0.152	-0.137	-0.144	-0.136	-0.146
4340	1.045	1.129	1.063	1.070	0.579	0.885	0.934	1.113	1.158	1.172	1.070	---
4464	-0.128	-0.168	-0.165	-0.150	-0.176	-0.168	-0.177	-0.156	-0.133	-0.143	-0.135	-0.144
4566	-0.106	-0.111	-0.110	-0.105	-0.161	-0.127	-0.149	-0.119	-0.104	-0.096	-0.108	-0.108
4673	-0.066	-0.085	-0.091	-0.078	-0.142	-0.107	-0.122	-0.085	-0.073	-0.086	-0.082	-0.081
4785	-0.048	-0.076	-0.072	-0.061	-0.099	-0.089	-0.088	-0.082	-0.075	-0.074	-0.069	-0.064
4861	0.736	1.071	1.042	0.844	0.806	1.060	1.107	1.108	1.009	1.078	0.975	---
4935	-0.021	-0.045	-0.044	-0.033	-0.050	-0.025	-0.045	-0.043	-0.023	-0.036	-0.027	-0.026
4975	0.003	-0.031	-0.028	-0.029	-0.050	-0.026	-0.030	-0.027	-0.027	-0.031	-0.018	-0.017
5000	0.000	0.000	0.000	0.000	0.000	0.000	0.000	0.000	0.000	0.000	0.000	0.000
5060	0.027	-0.013	0.001	-0.007	-0.035	0.000	-0.011	-0.007	-0.002	-0.005	-0.003	0.005
5128	0.053	0.044	0.047	0.036	0.012	0.030	0.032	0.052	0.059	0.056	0.037	0.051
5200	0.087	0.052	0.066	0.076	0.050	0.049	0.036	0.070	0.087	0.083	0.058	0.077
5232	0.089	0.074	0.091	0.079	0.082	0.080	0.085	0.095	0.083	0.090	0.071	0.093
5264	0.090	0.075	0.092	0.077	0.065	0.078	0.069	0.112	0.100	0.097	0.083	0.077
5360	0.084	0.072	0.078	0.078	0.066	0.070	0.068	0.068	0.076	0.082	0.076	0.082
5470	0.107	0.096	0.096	0.099	0.047	0.078	0.075	0.097	0.092	0.105	0.097	0.098
5556	0.111	0.109	0.106	0.106	0.078	0.096	0.091	0.087	0.111	0.114	0.102	0.106
5700	0.131	0.116	0.106	0.109	0.087	0.120	0.113	0.116	0.129	0.138	0.122	0.124
5800	0.151	0.175	0.161	0.162	0.138	0.164	0.150	0.151	0.174	0.183	0.161	0.168
5840	0.149	0.148	0.150	0.144	0.108	0.134	0.128	0.136	0.156	0.160	0.149	0.149
5875	0.185	0.162	0.171	0.165	0.153	0.156	0.152	0.152	0.156	0.175	0.148	0.167
6020	0.205	0.189	0.186	0.195	0.138	0.165	0.172	0.168	0.194	0.183	0.195	0.187
6058	0.212	0.197	0.194	0.194	0.166	0.186	0.184	0.190	0.191	0.190	0.199	0.197
6220	0.248	0.225	0.236	0.224	0.195	0.217	0.218	0.216	0.232	0.233	0.230	0.230
6300	0.255	0.246	0.245	0.250	0.204	0.234	0.233	0.229	0.258	0.247	0.249	0.246
6370	0.276	0.251	0.254	0.264	0.228	0.241	0.237	0.243	0.260	0.266	0.252	0.254
6440	0.297	0.270	0.276	0.271	0.239	0.267	0.263	0.267	0.284	0.285	0.283	0.277
6563	0.941	0.804	0.793	0.880	0.468	0.611	0.621	0.746	0.873	0.852	0.805	---
6650	0.315	0.292	0.287	0.302	0.251	0.284	0.283	0.291	0.310	0.315	0.292	0.297
6710	0.311	0.303	0.299	0.310	0.269	0.294	0.293	0.294	0.320	0.315	0.302	0.304
6792	0.333	0.313	0.308	0.318	0.282	0.296	0.308	0.300	0.343	0.325	0.326	0.315
7102	0.379	0.367	0.376	0.369	0.340	0.362	0.352	0.366	0.372	0.373	0.370	0.364
7530	---	---	---	---	0.427	0.436	0.447	0.447	0.472	0.469	0.457	0.451
7850	---	---	---	---	0.466	0.477	0.485	0.474	0.503	0.505	0.482	0.493
u-b	1.466	1.471	1.457	1.456	1.458	1.461	1.474	1.450	1.423	1.436	1.453	1.451
b-y	-0.019	-0.027	-0.032	-0.020	-0.046	-0.036	-0.054	-0.029	-0.021	-0.033	-0.022	-0.024
Δa	0.025	0.022	0.032	0.026	0.036	0.023	0.024	0.041	0.036	0.035	0.020	0.028
Δa'	0.035	0.037	0.051	0.031	0.060	0.054	0.048	0.083	0.057	0.053	0.040	0.033
Δι	-0.008	0.006	0.020	0.002	0.044	0.007	0.014	0.018	-0.003	-0.003	-0.004	0.013
Δι*	0.021	0.029	0.045	0.027	0.075	0.028	0.036	0.040	0.012	0.017	0.012	0.030

TABLE IX. — *Continuous energy distributions (− 2.5 log F_ν/F_{5000}) for CQ UMa.*

λ(Å)	1	2	3	4	5	6	7	8	9	10	11
3390	1.224	---	1.241	1.235	1.246	1.242	1.257	1.228	1.198	1.212	1.242
3448	1.197	---	1.199	1.206	1.201	1.217	1.200	1.188	1.178	1.201	1.191
3509	1.156	---	1.170	1.172	1.180	1.181	1.160	1.160	1.132	1.119	1.162
3571	1.154	---	1.151	1.155	1.162	1.167	1.150	1.153	1.143	1.133	1.140
3636	1.101	---	1.120	1.120	1.118	1.130	1.115	1.127	1.114	1.098	1.131
4032	-0.121	-0.086	0.002	-0.092	-0.028	-0.072	-0.096	-0.010	-0.077	-0.122	0.003
4167	-0.079	-0.030	-0.007	-0.065	-0.021	-0.048	-0.081	-0.013	-0.064	-0.094	-0.008
4255	-0.098	---	-0.013	-0.082	-0.037	-0.060	-0.077	-0.026	-0.076	---	-0.016
4464	-0.087	-0.083	-0.046	-0.074	-0.058	-0.083	-0.078	-0.061	-0.079	---	-0.051
4566	-0.078	-0.081	-0.040	-0.071	-0.058	-0.067	-0.063	-0.048	-0.049	-0.067	-0.034
4785	-0.082	-0.063	-0.048	-0.069	-0.058	-0.056	-0.072	-0.055	-0.063	-0.073	-0.047
5000	0.000	0.000	0.000	0.000	0.000	0.000	0.000	0.000	0.000	0.000	0.000
5263	0.095	0.079	0.065	0.096	0.067	0.067	0.081	0.077	0.079	0.085	0.076
5556	0.090	0.054	0.074	0.082	0.056	0.070	0.079	0.057	0.075	0.080	0.063
5840	0.104	0.109	0.095	0.118	0.093	0.110	0.098	0.102	0.128	0.115	0.100
6055	0.148	0.110	0.143	0.160	0.131	0.138	0.137	0.132	0.147	0.146	0.134
6370	0.225	0.197	0.194	0.222	0.198	0.206	0.199	0.176	0.201	0.191	0.175
6800	0.292	0.278	0.249	0.283	0.245	0.265	0.246	0.230	0.262	0.245	0.229
7100	0.319	0.312	0.294	0.320	0.294	0.313	0.301	0.275	0.304	0.299	0.278
7530	0.421	0.401	0.383	0.399	0.392	0.390	0.391	0.360	0.385	0.382	0.356
7850	0.476	0.446	0.406	0.438	0.413	0.425	0.408	0.392	0.451	0.401	0.388
u-b	1.389	---	1.371	1.392	1.390	1.393	1.403	1.371	1.348	---	1.370
b-y	---	---	0.042	-0.003	0.037	0.024	0.009	0.038	0.022	---	0.047
Δa	0.030	0.027	0.012	0.031	0.019	0.016	0.023	0.023	0.021	0.025	0.021
Δa'	---	0.046	0.028	0.069	0.037	0.031	0.062	0.042	0.039	0.059	0.036
Δ_1**	0.009	---	-0.007	0.003	-0.002	0.010	0.000	-0.003	-0.004	---	-0.007

λ(Å)	12	13	14	15	16	17	18	19	20	21	22	Average
3300	1.255	1.241	1.242	1.236	1.229	1.228	1.222	1.217	1.223	1.240	1.234	1.230
3390	1.258	1.233	1.238	1.217	1.236	1.252	1.239	1.232	1.232	1.258	1.235	1.236
3448	1.210	1.212	1.205	1.198	1.189	1.219	1.208	1.207	1.209	1.216	1.210	1.203
3509	1.164	1.165	1.177	1.150	1.158	1.173	1.163	1.150	1.148	1.166	1.148	1.160
3540	1.164	1.153	1.152	1.141	1.160	1.161	1.138	1.138	1.138	1.140	1.155	1.146
3571	1.164	1.166	1.172	1.159	1.146	1.177	1.168	1.154	1.157	1.173	1.163	1.157
3636	1.132	1.137	1.145	1.116	1.108	1.128	1.121	1.111	1.115	1.117	1.129	1.120
3704	1.106	1.110	1.102	1.111	1.102	1.095	1.083	1.089	1.079	1.101	1.095	1.095
4032	-0.013	-0.054	-0.060	-0.084	-0.038	-0.109	-0.111	-0.119	-0.079	-0.055	-0.056	-0.067
4167	-0.001	-0.038	-0.042	-0.047	0.006	-0.066	-0.075	-0.076	-0.035	-0.042	-0.027	-0.043
4200	0.006	-0.029	-0.028	-0.049	0.003	-0.058	-0.072	-0.087	-0.047	-0.027	-0.028	-0.040
4255	-0.015	-0.020	-0.048	-0.060	0.000	-0.076	-0.079	-0.084	-0.058	-0.052	-0.043	-0.051
4340	0.655	0.671	0.690	0.664	0.664	0.661	0.653	0.667	0.665	0.649	0.675	0.665
4464	-0.066	-0.060	-0.072	-0.096	-0.064	-0.095	-0.079	-0.096	-0.075	-0.083	-0.072	-0.074
4566	-0.063	-0.062	-0.078	-0.086	-0.067	-0.069	-0.073	-0.077	-0.089	-0.060	-0.063	-0.066
4673	-0.049	-0.059	-0.071	-0.080	-0.069	-0.058	-0.069	-0.056	-0.077	-0.048	-0.058	-0.059
4785	-0.066	-0.062	-0.060	-0.076	-0.067	-0.068	-0.073	-0.072	-0.068	-0.072	-0.055	-0.065
4861	0.622	0.643	0.659	0.649	0.603	0.632	0.605	0.634	0.605	0.621	0.625	0.629
4935	-0.036	-0.033	-0.020	-0.032	-0.036	-0.015	-0.021	-0.039	-0.049	-0.041	-0.041	-0.032
4975	-0.022	-0.021	-0.021	-0.027	-0.027	-0.033	-0.028	-0.035	-0.039	-0.049	-0.033	-0.030
5000	0.000	0.000	0.000	0.000	0.000	0.000	0.000	0.000	0.000	0.000	0.000	0.000
5060	-0.020	-0.014	0.003	-0.024	-0.017	0.004	-0.013	-0.023	-0.034	-0.024	-0.033	-0.017
5128	0.017	0.033	0.041	0.009	0.014	0.026	0.013	0.012	0.000	0.024	0.012	0.018
5200	0.058	0.063	0.072	0.059	0.057	0.092	0.076	0.074	0.051	0.067	0.062	0.069
5232	0.074	0.076	0.077	0.076	0.050	0.095	0.076	0.087	0.052	0.045	0.054	0.073
5264	0.070	0.068	0.070	0.066	0.060	0.086	0.080	0.081	0.060	0.070	0.064	0.075
5360	0.042	0.050	0.049	0.044	0.030	0.069	0.058	0.048	0.045	0.042	0.034	0.050
5470	0.043	0.043	0.055	0.044	0.040	0.070	0.073	0.063	0.053	0.062	0.042	0.056
5556	0.068	0.072	0.074	0.069	0.038	0.079	0.075	0.071	0.066	0.057	0.048	0.068
5700	0.073	0.083	0.092	0.079	0.053	0.093	0.089	0.089	0.065	0.076	0.062	0.081
5800	0.094	0.116	0.118	0.117	0.089	0.142	0.124	0.133	0.129	0.118	0.103	0.121
5840	0.086	0.099	0.105	0.102	0.077	0.112	0.106	0.107	0.098	0.098	0.084	0.102
5875	0.090	0.121	0.123	0.125	0.108	0.120	0.127	0.125	0.118	0.111	0.103	0.118
6020	0.119	0.137	0.130	0.130	0.118	0.146	0.146	0.128	0.134	0.131	0.131	0.135
6058	0.127	0.150	0.152	0.152	0.139	0.154	0.146	0.145	0.137	0.151	0.124	0.141
6220	0.160	0.179	0.169	0.168	0.146	0.190	0.182	0.180	0.153	0.166	0.159	0.170
6300	0.173	0.188	0.183	0.186	0.162	0.203	0.198	0.184	0.184	0.176	0.181	0.185
6370	0.177	0.189	0.204	0.181	0.169	0.213	0.221	0.206	0.193	0.192	0.191	0.196
6440	0.203	0.232	0.231	0.224	0.190	0.240	0.237	0.242	0.220	0.225	0.205	0.225
6563	0.514	0.567	0.556	0.564	0.538	0.592	0.584	0.584	0.549	0.556	0.543	0.561
6650	0.214	0.221	0.236	0.236	0.215	0.264	0.257	0.247	0.221	0.236	0.213	0.235
6710	0.213	0.231	0.240	0.229	0.214	0.258	0.253	0.252	0.220	0.233	0.219	0.235
6792	0.240	0.248	0.254	0.259	0.223	0.281	0.264	0.255	0.252	0.255	0.248	0.255
7102	0.267	0.282	0.300	0.303	0.270	0.305	0.311	0.319	0.296	0.278	0.284	0.297
7530	0.352	0.377	0.394	0.392	0.354	0.404	0.396	0.389	0.363	0.365	0.370	0.383
7850	0.393	0.410	0.421	0.423	0.397	0.436	0.423	0.418	0.390	0.431	0.393	0.417
u-b	1.385	1.382	1.394	1.391	1.377	1.388	1.384	1.374	1.386	1.381	1.375	1.376
b-y	0.047	0.040	0.025	0.021	0.050	0.017	0.015	0.025	0.024	0.043	0.053	0.033
Δa	0.030	0.031	0.029	0.031	0.027	0.039	0.031	0.038	0.025	0.029	0.031	0.033
Δa'	0.045	0.036	0.036	0.042	0.039	0.054	0.054	0.052	0.033	0.043	0.033	0.043
Δ_1	0.009	-0.004	0.011	0.016	0.016	0.023	0.014	0.012	0.020	0.011	0.014	0.009
Δ_1*	0.034	0.017	0.028	0.040	0.047	0.039	0.021	0.023	0.034	0.028	0.027	0.024
Δ_1**	0.012	0.009	0.008	0.024	0.037	0.022	0.011	0.018	0.019	0.006	0.013	0.010
hb	0.673	0.691	0.699	0.703	0.655	0.674	0.652	0.690	0.664	0.678	0.673	---

TABLE X. — *Continuous energy distributions (− 2.5 log F_ν/F_{5000}) for CU VIR.*

λ(Å)	32	33	34	35	36	37	38	39	40	41	42	43	44	45
3300	0.493	0.428	0.412	0.491	0.506	0.492	0.491	0.473	0.490	0.508	0.536	0.476	0.486	0.497
3390	0.501	0.442	0.415	0.497	0.500	0.494	0.492	0.479	0.502	0.519	0.528	0.477	0.478	0.495
3448	0.507	0.453	0.427	0.504	0.503	0.500	0,498	0.494	0.507	0.508	0.555	0.487	0.480	0.495
3509	0.507	0.440	0.431	0.502	0.506	0.492	0.488	0.481	0.496	0.505	0.520	0.478	0.484	0.499
3540	---	0.466	0.427	0.502	0.512	0.497	0.495	0.488	0.504	0.506	0.507	0.478	0.487	0.500
3571	0.519	0.452	0.431	0.528	0.530	0.512	0.512	0.502	0.510	0.525	0.526	0.486	0.499	0.512
3636	0.515	0.447	0.426	0.508	0.521	0.499	0.501	0.487	0.491	0.514	0.551	0.480	0.491	0.496
3704	0.512	0.451	0.435	0.509	0.506	0.504	0.498	0.488	0.488	0.517	0.519	0.469	0.491	0.490
4032	-0.280	-0.304	-0.304	-0.293	-0.299	-0.302	-0.297	-0.310	-0.315	-0.298	-0.282	-0.287	-0.282	-0.275
4167	-0.246	-0.250	-0.249	-0.258	-0.247	-0.255	-0.266	-0.259	-0.241	-0.233	-0.225	-0.218	-0.234	-0.245
4200	-0.255	-0.217	-0.213	-0.230	-0.232	-0.231	-0.238	-0.232	-0.224	-0.220	-0.214	-0.194	-0.204	-0.216
4255	-0.215	-0.231	-0.218	-0.209	-0.222	-0.230	-0.230	-0.230	-0.217	-0.219	-0.199	-0.203	-0.204	-0.221
4340	---	0.312	0.300	0.353	0.355	0.348	0.327	0.340	0.344	0.362	0.382	0.345	0.320	0.329
4464	-0.168	-0.214	-0.213	-0.196	-0.195	-0.197	-0.202	-0.208	-0.176	-0.176	-0.169	-0.165	-0.170	-0.164
4566	-0.141	-0.152	-0.150	-0.154	-0.149	-0.162	-0.162	-0.145	-0.157	-0.154	-0.135	-0.128	-0.132	-0.144
4673	-0.110	-0.100	-0.116	-0.124	-0.107	-0.101	-0.105	-0.100	-0.122	-0.111	-0.094	-0.082	-0.093	-0.097
4785	-0.074	-0.087	-0.084	-0.085	-0.092	-0.095	-0.082	-0.087	-0.094	-0.077	-0.072	-0.062	-0.070	-0.078
4861	---	0.431	0.410	0.460	0.457	0.463	0.458	0.450	0.440	0.464	0.473	0.405	0.401	0.416
4935	-0.033	-0.038	-0.042	-0.031	-0.030	-0.034	-0.027	-0.033	-0.039	-0.040	-0.028	-0.019	-0.027	-0.034
4975	---	-0.030	-0.028	-0.023	-0.019	-0.019	-0.013	-0.025	-0.037	-0.026	-0.022	-0.014	-0.022	-0.027
5000	0.000	0.000	0.000	0.000	0.000	0.000	0.000	0.000	0.000	0.000	0.000	0.000	0.000	0.000
5060	---	0.026	0.033	0.014	0.028	0.035	0.026	0.039	0.023	0.028	0.042	0.037	0.031	0.017
5128	0.021	0.046	0.037	0.039	0.050	0.038	0.032	0.052	0.028	0.045	0.063	0.044	0.041	0.028
5200	0.063	0.091	0.085	0.062	0.063	0.062	0.079	0.074	0.059	0.065	0.073	0.081	0.067	0.065
5232	---	0.101	0.097	0.061	0.086	0.074	0.089	0.095	0.073	0.070	0.094	0.087	0.075	0.068
5264	0.062	0.076	0.078	0.060	0.066	0.062	0.072	0.079	0.048	0.064	0.080	0.080	0.066	0.060
5360	0.086	0.096	0.082	0.085	0.094	0.093	0.095	0.095	0.070	0.082	0.082	0.094	0.098	0.088
5470	0.103	0.097	0.111	0.112	0.113	0.125	0.131	0.129	0.109	0.110	0.111	0.137	0.123	0.111
5556	0.125	0.126	0.121	0.131	0.144	0.141	0.136	0.136	0.123	0.117	0.136	0.129	0.136	0.127
5700	0.160	0.166	0.159	0.156	0.164	0.170	0.174	0.175	0.152	0.153	0.176	0.174	0.174	0.169
5800	---	0.203	0.199	0.207	0.209	0.210	0.226	0.220	0.185	0.206	0.200	0.204	0.203	0.207
5840	0.191	0.204	0.181	0.175	0.206	0.204	0.214	0.198	0.186	0.185	0.211	0.191	0.190	0.183
5875	---	0.229	0.211	0.216	0.243	0.233	0.223	0.232	0.201	0.207	0.223	0.215	0.215	0.211
6020	0.242	0.235	0.237	0.247	0.229	0.243	0.255	0.246	0.226	0.223	0.239	0.255	0.241	0.220
6058	---	0.252	0.244	0.250	0.257	0.263	0.255	0.265	0.244	0.252	0.261	0.254	0.255	0.242
6220	0.288	0.297	0.298	0.296	0.294	0.301	0.304	0.300	0.281	0.302	0.294	0.290	0.289	0.280
6300	0.306	0.319	0.304	0.314	0.308	0.321	0.318	0.327	0.299	0.307	0.301	0.324	0.312	0.298
6370	0.328	0.349	0.337	0.322	0.329	0.331	0.350	0.345	0.303	0.327	0.317	0.330	0.317	0.327
6440	---	0.358	0.367	0.339	0.344	0.351	0.365	0.359	0.334	0.348	0.345	0.360	0.367	0.329
6563	---	0.573	0.562	0.591	0.593	0.588	0.602	0.602	0.597	0.608	0.603	0.587	0.585	0.575
6650	0.372	0.376	0.365	0.377	0.395	0.361	0.386	0.396	0.370	0.371	0.389	0.380	0.377	0.378
6710	---	0.383	0.375	0.386	0.384	0.381	0.394	0.405	0.370	0.383	0.396	0.394	0.373	0.379
6792	0.404	0.417	0.392	0.398	0.389	0.425	0.411	0.406	0.373	0.400	0.407	0.404	0.397	0.400
7102	0.462	0.475	0.463	0.469	0.462	0.468	0.482	0.469	0.467	0.465	0.476	0.477	0.454	0.439
7530	---	0.571	0.567	0.559	0.569	0.569	0.583	0.580	0.546	0.561	0.578	0.577	0.546	0.533
7850	---	0.627	0.631	0.606	0.618	0.625	0.630	0.630	0.591	0.602	0.610	0.636	0.604	0.594
u-b	0.744	0.684	0.670	0.754	0.753	0.742	0.740	0.724	0.749	0.755	0.762	0.698	0.713	0.731
b-y	-0.056	-0.064	-0.070	-0.073	-0.073	-0.076	-0.079	-0.074	-0.064	-0.061	-0.055	-0.054	-0.058	-0.055
Δa	0.010	0.031	0.027	0.009	0.012	0.006	0.015	0.018	0.009	0.014	0.019	0.014	0.008	0.010
Δa'	0.007	0.023	0.034	0.020	0.016	0.015	0.014	0.030	0.007	0.014	0.014	0.018	0.009	0.010
Δι	0.007	0.029	0.026	0.003	0.017	0.019	0.008	0.021	0.029	0.027	0.016	0.034	0.019	0.012
Δι*	0.010	0.050	0.054	0.028	0.035	0.036	0.028	0.042	0.038	0.034	0.027	0.041	0.029	0.010
hb	---	0.494	0.473	0.518	0.518	0.528	0.513	0.510	0.507	0.523	0.523	0.446	0.450	0.472

TABLE X *(continued)*.

λ(Å)	46	47	48	49	Average (32-49)	Total Average[1]
3300	0.523	0.431	0.455	0.458	0.480	0.483
3390	0.524	0.442	0.481	0.470	0.485	0.488
3448	0.522	0.446	0.482	0.472	0.491	0.494
3509	0.528	0.446	0.461	0.467	0.485	0.490
3540	0.521	0.448	0.463	0.470	0.485	0.489
3571	0.534	0.459	0.480	0.479	0.500	0.503
3636	0.526	0.441	0.459	0.462	0.490	0.495
3704	0.514	0.440	0.457	0.469	0.486	0.491
4032	-0.272	-0.282	-0.270	-0.271	-0.290	-0.284
4167	-0.236	-0.236	-0.231	-0.233	-0.242	-0.245
4200	-0.212	-0.192	-0.202	-0.202	-0.217	-0.220
4255	-0.207	-0.214	-0.199	-0.204	-0.215	-0.219
4340	0.349	0.301	0.306	0.314	---	---
4464	-0.175	-0.180	-0.170	-0.176	-0.184	-0.185
4566	-0.135	-0.147	-0.124	-0.124	-0.144	-0.142
4673	-0.097	-0.101	-0.084	-0.102	-0.103	-0.103
4785	-0.070	-0.080	-0.068	-0.078	-0.080	-0.078
4861	0.429	0.397	0.398	0.411	---	---
4935	-0.023	-0.034	-0.021	-0.022	-0.031	-0.030
4975	-0.015	-0.018	-0.023	-0.019	-0.022	-0.022
5000	0.000	0.000	0.000	0.000	0.000	0.000
5060	0.036	0.029	0.042	0.042	0.031	0.020
5128	0.035	0.047	0.047	0.048	0.041	0.041
5200	0.069	0.084	0.086	0.080	0.073	0.074
5232	0.080	0.084	0.094	0.077	0.083	0.085
5264	0.080	0.084	0.084	0.076	0.071	0.074
5360	0.097	0.100	0.110	0.102	0.092	0.093
5470	0.121	0.129	0.122	0.122	0.118	0.119
5556	0.140	0.120	0.133	0.123	0.130	0.130
5700	0.177	0.148	0.151	0.152	0.164	0.164
5800	0.214	0.210	0.215	0.207	0.207	0.208
5840	0.193	0.186	0.214	0.188	0.194	0.195
5875	0.226	0.206	0.224	0.216	0.219	0.219
6020	0.241	0.236	0.237	0.241	0.238	0.238
6058	0.258	0.251	0.254	0.246	0.253	0.251
6220	0.287	0.279	0.289	0.282	0.292	0.291
6300	0.318	0.319	0.327	0.303	0.312	0.312
6370	0.344	0.326	0.351	0.333	0.331	0.332
6440	0.355	0.344	0.370	0.345	0.352	0.355
6563	0.610	0.572	0.584	0.573	---	---
6650	0.382	0.369	0.382	0.363	0.377	0.379
6710	0.396	0.375	0.383	0.384	0.385	0.388
6792	0.411	0.409	0.420	0.400	0.403	0.406
7102	0.465	0.455	0.455	0.451	0.464	0.462
7530	0.577	0.554	0.554	0.547	0.563	0.564
7850	0.615	0.599	0.610	0.610	0.614	0.615
u-b	0.754	0.680	0.688	0.698	0.725	0.727
b-y	-0.063	-0.069	-0.056	-0.060	-0.065	-0.065
Δa	0.012	0.022	0.021	0.015	0.016	0.018
Δa'	0.022	0.036	0.015	0.025	0.019	0.020
Δι	0.011	0.030	0.013	0.015	0.018	0.014
Δι*	0.024	0.043	0.025	0.029	0.033	0.027
hb	0.476	0.454	0.443	0.461	---	---

Note: [1]Additional value: λ4722, m = 0.090.

TABLE XI. — *Continuous energy distributions (− 2.5 log F_v/F_{5000}) for CS Vir.*

λ(Å)	1	2	3	4	5
3390	1.086	1.068	1.072	1.121	1.108
3448	1.113	1.058	1.029	1.115	1.110
3509	1.075	1.012	1.008	1.081	1.079
3571	1.065	1.035	0.999	1.072	1.053
3636	1.032	1.006	0.964	1.035	1.041
4032	-0.161	-0.220	-0.225	-0.107	-0.088
4167	-0.111	-0.148	-0.163	-0.099	-0.070
4255	-0.095	-0.110	-0.124	-0.077	-0.064
4464	-0.032	-0.123	-0.113	-0.102	-0.080
4566	-0.106	-0.098	-0.081	-0.100	-0.097
4785	-0.082	-0.081	-0.079	-0.086	-0.089
5000	0.000	0.000	0.000	0.000	0.000
5263	0.133	0.127	0.158	0.094	0.086
5556	0.097	0.174	0.138	0.085	0.063
5840	0.121	0.168	0.169	0.126	0.117
6055	0.176	0.221	0.214	0.179	0.175
6370	0.252	0.305	0.276	0.247	0.232
6800	0.328	0.344	0.318	0.319	0.303
7100	0.386	0.395	0.360	0.354	0.363
7530	0.436	0.490	0.517	0.469	0.440
7850	0.463	0.538	0.492	0.490	0.504
u-b	1.286	1.259	1.245	1.310	1.300
b-y	-0.053	-0.090	-0.073	-0.027	-0.010
Δa	0.050	0.030	0.054	0.031	0.031
Δa'	0.108	0.098	0.125	0.076	0.071
Δι**	0.048	0.063	0.044	0.013	0.011

λ(Å)	6	7	8	9	10
3390	1.117	1.094	1.107	1.135	1.123
3448	1.096	1.078	1.072	1.114	1.113
3509	1.082	1.042	1.031	1.090	1.080
3571	1.068	1.026	1.030	1.059	1.051
3636	1.030	1.001	0.990	1.032	1.020
4032	-0.121	-0.197	-0.193	-0.133	-0.078
4167	-0.093	-0.167	-0.177	-0.114	-0.088
4255	-0.075	-0.116	-0.115	-0.088	-0.073
4464	-0.085	-0.124	-0.137	-0.116	-0.109
4566	-0.093	-0.081	-0.080	-0.100	-0.111
4785	-0.087	-0.065	-0.075	-0.092	-0.098
5000	0.000	0.000	0.000	0.000	0.000
5263	0.106	0.131	0.121	0.082	0.103
5556	0.080	0.149	0.154	0.082	0.080
5840	0.125	0.170	0.177	0.114	0.130
6055	0.188	0.212	0.221	0.165	0.181
6370	0.252	0.271	0.270	0.222	0.226
6800	0.307	0.314	0.319	0.291	0.282
7100	0.363	0.379	0.368	0.359	0.332
7530	0.446	0.449	0.467	0.437	0.422
7850	0.478	0.477	0.483	0.446	0.450
u-b	1.305	1.262	1.273	1.323	1.318
b-y	-0.026	-0.062	-0.065	-0.023	-0.040
Δa	0.039	0.036	0.029	0.024	0.038
Δa'	0.089	0.089	0.091	0.072	0.093
Δι**	0.018	0.030	0.029	0.020	0.008

TABLE XI *(continued)*.

λ(Å)	11	12	13	14	Average
3300	1.018	1.092	1.089	1.084	1.090
3390	1.018	1.091	1.111	1.076	1.095
3448	1.016	1.098	1.092	1.077	1.084
3509	0.963	1.040	1.050	1.039	1.048
3540	0.952	1.040	1.034	1.022	1.031
3571	0.974	1.034	1.036	1.044	1.039
3636	0.948	1.001	1.006	0.995	1.007
3704	0.927	0.978	0.968	0.974	0.986
4032	-0.248	-0.192	-0.163	-0.209	-0.167
4167	-0.194	-0.154	-0.125	-0.161	-0.133
4200	-0.138	-0.106	-0.075	-0.118	0.087
4255	-0.136	-0.125	-0.101	-0.119	-0.101
4340	0.550	0.583	0.556	0.585	0.590
4464	-0.176	-0.151	-0.114	-0.141	-0.122
4566	-0.120	-0.136	-0.115	-0.117	-0.103
4673	-0.105	-0.117	-0.103	-0.096	-0.089
4785	-0.103	-0.117	-0.098	-0.092	-0.089
4861	0.626	0.608	0.542	0.604	0.605
4935	-0.076	-0.065	-0.058	-0.060	-0.058
4975	-0.050	-0.057	-0.061	-0.052	-0.051
5000	0.000	0.000	0.000	0.000	0.000
5060	0.000	-0.017	-0.019	-0.007	-0.007
5128	0.043	0.043	0.048	0.040	0.052
5200	0.100	0.079	0.090	0.097	0.104
5232	0.119	0.083	0.098	0.097	0.115
5264	0.096	0.070	0.078	0.097	0.106
5360	0.108	0.063	0.082	0.090	0.102
5470	0.087	0.064	0.075	0.093	0.091
5556	0.130	0.082	0.090	0.102	0.108
5700	0.098	0.091	0.101	0.103	0.106
5800	0.150	0.142	0.152	0.158	0.160
5840	0.126	0.119	0.131	0.136	0.138
5875	0.146	0.145	0.144	0.156	0.157
6020	0.151	0.168	0.169	0.175	0.175
6058	0.172	0.176	0.177	0.195	0.189
6220	0.228	0.211	0.206	0.218	0.224
6300	0.238	0.238	0.232	0.238	0.242
6370	0.256	0.232	0.251	0.258	0.254
6440	0.287	0.280	0.277	0.301	0.291
6563	0.582	0.599	0.585	0.603	0.596
6650	0.274	0.302	0.301	0.304	0.299
6710	0.264	0.294	0.301	0.303	0.294
6792	0.303	0.314	0.309	0.310	0.312
7102	0.358	0.350	0.354	0.365	0.363
7530	0.457	0.443	0.457	0.454	0.456
7850	0.501	0.508	0.493	0.520	0.489
u-b	1.238	1.312	1.296	1.283	1.283
b-y	-0.069	-0.037	-0.031	-0.041	-0.038
Δa	0.052	0.044	0.048	0.048	0.056
Δa'	0.088	0.068	0.060	0.075	0.080
Δι	0.022	0.022	0.026	0.018	0.018
Δι*	0.072	0.057	0.052	0.052	0.049
Δι**	0.060	0.035	0.027	0.041	0.030
hb	0.716	0.699	0.620	0.680	---

TABLE XII. — *Continuous energy distributions ($-2.5 \log F_\nu/F_{5000}$) for β CrB.*

λ(Å)	1	2	3	4	5	6	7	8
3390	1.436	1.466	1.449	1.408	---	---	---	1.457
3448	1.434	1.450	1.444	1.426	---	---	---	1.425
3509	1.360	1.368	1.366	1.339	1.354	1.319	---	1.361
3571	1.385	1.387	1.369	1.371	1.382	1.363	---	1.355
3636	1.318	1.323	1.307	1.293	1.277	1.292	---	1.297
4032	0.098	0.125	0.093	0.088	0.098	0.093	0.112	0.054
4167	0.120	0.124	0.084	0.063	0.087	0.081	0.102	0.100
4255	0.081	0.126	0.084	0.082	0.058	0.049	0.083	0.097
4464	-0.005	0.037	0.024	0.006	-0.020	-0.023	0.012	-0.002
4566	-0.042	-0.027	-0.014	-0.055	-0.056	-0.057	-0.040	-0.012
4785	-0.078	-0.076	-0.066	-0.086	-0.078	-0.078	-0.072	-0.074
5000	0.000	0.000	0.000	0.000	0.000	0.000	0.000	0.000
5263	0.077	0.051	0.067	0.035	0.036	0.021	0.049	0.039
5556	0.000	-0.029	-0.003	-0.024	-0.020	-0.030	-0.006	-0.001
5840	-0.018	-0.047	-0.001	-0.025	-0.030	-0.033	-0.022	-0.021
6055	0.001	-0.020	0.026	0.004	0.003	-0.005	0.003	0.009
6370	0.039	0.043	0.062	0.031	0.017	0.021	0.049	0.050
6800	0.073	0.062	0.079	0.059	0.025	0.030	---	0.058
7100	0.113	0.088	0.124	0.098	0.059	0.076	---	0.098
7530	0.153	0.155	0.189	0.169	0.137	0 147	---	0.185
7850	0.197	0.194	0.209	0.182	0.167	0.173	---	0.187
u-b	1.573	1.583	1.557	1.553	---	---	---	1.563
b-y	0.069	0.109	0.096	0.091	0.081	0.090	0.089	0.106
Δa	0.038	0.030	0.031	0.020	0.022	0.018	0.024	0.016
Δa'	0.104	0.083	0.075	0.066	0.072	0.062	0.070	0.058

λ(Å)	9	10	11	12	13	14	15	16
3390	1.475	1.478	1.473	1.464	1.483	1.467	1.490	1.485
3448	1.448	1.446	1.435	1.433	1.450	1.445	1.462	1.467
3509	1.380	1.381	1.386	1.371	1.386	1.379	1.360	1.378
3571	1.350	1.355	1.356	1.348	1.356	1.350	1.344	1.356
3636	1.305	1.300	1.297	1.287	1.314	1.308	1.299	1.303
4032	0.054	0.106	0.102	0.095	0.122	0.123	0.113	0.113
4167	0.106	0.127	0.124	0.123	0.130	0.111	0.121	0.129
4255	0.105	0.113	0.115	0.117	0.131	0.115	0.119	0.108
4464	0.011	0.051	0.045	0.038	0.063	0.048	0.048	0.041
4566	-0.011	0.003	0.000	0.000	0.022	0.008	0.033	0.010
4785	-0.069	-0.061	-0.072	-0.073	-0.047	-0.060	-0.058	-0.057
5000	0.000	0.000	0.000	0.000	0.000	0.000	0.000	0.000
5263	0.049	0.055	0.068	0.056	0.059	0.056	0.064	0.063
5556	0.001	-0.004	-0.005	-0.014	0.008	0.004	0.008	0.010
5840	-0.012	-0.018	-0.018	-0.029	-0.014	-0.011	-0.004	-0.027
6055	0.010	0.009	0.002	-0.009	-0.001	0.003	0.010	-0.002
6370	0.045	0.046	0.041	0.030	0.028	0.031	0.048	0.031
6800	0.070	0.078	0.060	0.055	0.047	0.050	0.071	0.040
7100	0.115	0.118	0.102	0.095	0.091	0.102	0.111	0.089
7530	0.180	0.176	0.172	0.163	0.163	0.168	0.177	0.158
7850	0.204	0.213	0.221	0.194	0.201	0.188	0.214	0.198
u-b	1.575	1.564	1.569	1.559	1.555	1.555	1.549	1.561
b-y	0.104	0.115	0.104	0.113	0.123	0.112	0.120	0.108
Δa	0.021	0.023	0.033	0.027	0.022	0.022	0.025	0.025
Δa'	0.061	0.064	0.085	0.077	0.057	0.062	0.065	0.075

TABLE XII *(continued)*.

λ(Å)	17	18	19	20	21	22	23	24	25	26	27
3300	1.454	1.442	1.450	1.463	1.458	1.463	1.472	1.484	1.464	1.487	1.479
3390	1.437	1.434	1.437	1.436	1.439	1.459	1.456	1.471	1.454	1.469	1.446
3448	1.441	1.421	1.427	1.438	1.436	1.448	1.452	1.422	1.436	1.438	1.442
3509	1.365	1.352	1.358	1.365	1.365	1.370	1.358	1.407	1.395	1.412	1.372
3571	1.371	1.348	1.366	1.366	1.368	1.383	1.357	1.358	1.371	1.381	1.355
3636	1.304	1.299	1.304	1.309	1.306	1.313	1.299	1.310	1.319	1.345	1.308
3704	1.192	1.199	1.190	1.194	1.202	1.204	1.182	1.217	1.221	1.237	1.215
4032	0.121	0.122	0.119	0.108	0.114	0.116	0.086	0.098	0.104	0.106	0.108
4167	0.121	0.117	0.110	0.109	0.117	0.108	0.097	0.087	0.106	0.099	0.098
4200	0.129	0.128	0.117	0.117	0.114	0.119	0.119	0.108	0.131	0.122	0.114
4255	0.093	0.093	0.087	0.084	0.074	0.081	0.080	0.071	0.082	0.084	0.073
4464	0.009	0.011	0.006	-0.002	0.006	0.003	0.013	-0.012	0.008	0.001	0.006
4566	-0.022	-0.026	-0.020	-0.024	-0.016	-0.014	-0.015	-0.042	-0.034	-0.017	-0.019
4785	-0.066	-0.073	-0.067	-0.072	-0.072	-0.069	-0.070	-0.026	-0.046	-0.040	-0.060
5000	0.000	0.000	0.000	0.000	0.000	0.000	0.000	0.000	0.000	0.000	0.000
5128	-0.004	-0.026	-0.013	-0.019	-0.015	-0.012	-0.014	0.003	-0.011	-0.011	-0.011
5264	0.040	0.034	0.039	0.037	0.047	0.050	0.021	0.054	0.041	0.049	0.042
5360	-0.001	0.003	0.005	-0.001	0.003	0.006	0.012	0.018	0.007	0.014	0.009
5470	-0.022	-0.034	-0.023	-0.026	-0.020	-0.014	-0.024	-0.009	-0.013	-0.016	-0.018
5556	-0.014	-0.020	-0.007	-0.015	-0.008	0.003	-0.016	-0.018	-0.008	-0.011	-0.007
5840	-0.042	-0.024	-0.022	-0.030	-0.023	-0.019	-0.028	-0.029	-0.013	-0.029	-0.030
6020	-0.011	-0.017	-0.009	-0.005	-0.007	-0.006	-0.022	-0.004	0.007	-0.007	-0.014
6220	0.012	0.002	0.021	0.019	0.018	0.024	0.018	0.001	0.021	0.007	0.006
6370	0.026	0.021	0.026	0.025	0.031	0.033	0.024	0.027	0.045	0.026	0.018
6650	0.040	0.039	0.051	0.051	0.048	0.056	0.040	0.035	0.050	0.044	0.025
6792	0.042	0.040	0.050	0.044	0.043	0.054	0.029	0.046	0.049	0.036	0.032
7102	0.088	0.088	0.097	0.081	0.085	0.091	0.066	0.075	0.086	0.068	0.072
u-b	1.561	1.555	1.556	1.567	1.562	1.569	1.564	1.571	1.571	1.576	1.565
b-y	0.125	0.125	0.122	0.123	0.119	0.117	0.127	0.121	0.120	0.130	0.123
Δa	0.018	0.013	0.013	0.014	0.018	0.018	0.006	0.022	0.013	0.018	0.022
Δa'	0.072	0.068	0.069	0.070	0.076	0.075	0.040	0.050	0.041	0.053	0.056
Δι	-0.002	0.009	0.004	0.011	0.016	0.010	0.019	0.007	0.020	0.010	0.010
Δι*	0.025	0.013	0.010	0.018	0.010	0.016	0.019	0.013	0.020	0.010	0.007

λ(Å)	28	29	30	Average
3300	1.461	1.438	1.442	1.461
3390	1.438	1.448	1.442	1.455
3448	1.433	1.437	1.446	1.440
3509	1.361	1.356	1.360	1.371
3540	---	1.335	1.333	1.345
3571	1.359	1.347	1.345	1.361
3636	1.304	1.294	1.296	1.306
3704	1.210	1.206	1.213	1.203
4032	0.109	0.069	0.082	0.107
4167	0.092	0.091	0.091	0.108
4200	0.109	0.118	0.119	0.127
4255	0.070	0.092	0.095	0.095
4340	---	0.640	0.645	---
4464	-0.007	0.025	0.020	0.018
4566	-0.027	-0.024	-0.018	-0.015
4673	-0.014	-0.007	-0.010	-0.004
4785	-0.074	-0.081	-0.075	-0.071
4861	---	0.521	0.528	---
4935	-0.024	-0.029	-0.043	-0.027
4975	---	-0.072	-0.065	-0.066
5000	0.000	0.000	0.000	0.000
5060	---	-0.058	-0.044	-0.049
5128	-0.022	-0.025	-0.021	-0.012
5200	0.029	0.039	0.046	0.043
5232	---	0.058	0.050	0.055
5264	0.032	0.046	0.052	0.048
5360	-0.002	-0.018	-0.002	0.006
5470	-0.028	-0.016	-0.020	-0.018
5556	-0.023	-0.012	-0.019	-0.009
5700	-0.044	-0.019	-0.033	-0.025
5800	---	0.014	0.003	0.012
5840	-0.036	-0.035	-0.031	-0.024
5875	---	-0.004	-0.022	-0.009
6020	-0.010	-0.014	-0.008	-0.006
6058	---	0.000	-0.003	0.002
6220	0.014	0.013	0.023	0.017
6300	0.016	0.034	0.036	0.038
6370	0.019	0.034	0.031	0.033
6440	---	0.070	0.069	0.071
6563	---	0.363	0.359	---
6650	0.036	0.064	0.059	0.050
6710	---	0.054	0.039	0.047
6792	0.034	0.052	0.055	0.050
7102	0.086	0.089	0.091	0.091
7530	---	0.159	0.153	0.165
7850	---	0.184	0.182	0.195
u-b	1.560	1.538	1.540	1.544
b-y	0.141	0.138	0.138	0.138
Δa	0.020	0.039	0.041	0.039
Δa'	0.068	0.072	0.073	0.064
Δι	0.006	0.019	0.012	0.012
Δι*	0.003	0.035	0.031	0.032

Note: Scan 7 has the additional values: λ6896, m=0.047; λ7142, m=0.109; λ7272, m=0.110; λ7408, m=0.156.

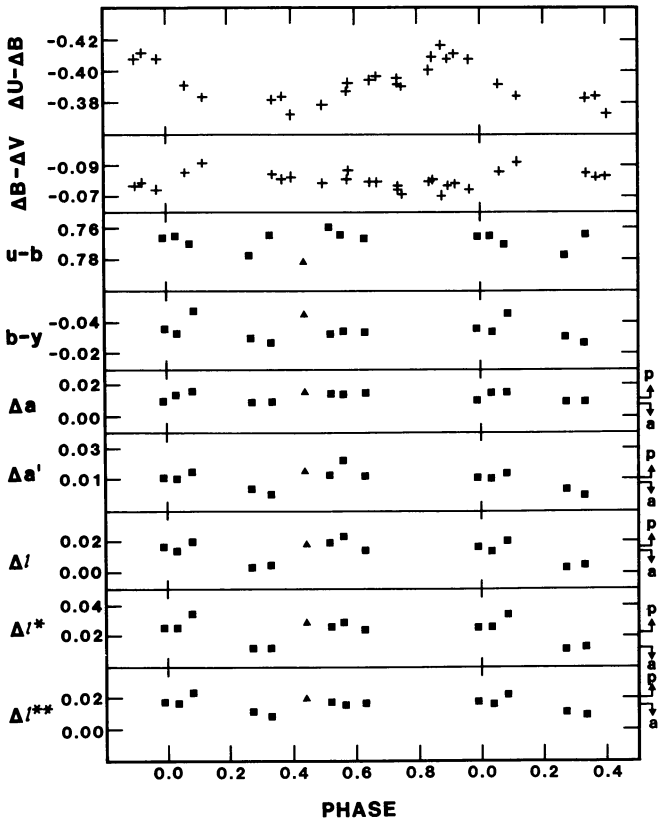

FIGURE 1. — Index values of 63 And as a function of phase. Pluses represent *UBV* photometry of Winzer (1974), closed squares are spectrophotometric values of SJA and closed triangles, spectrophotometric values of DMP/SJA (see Table II).

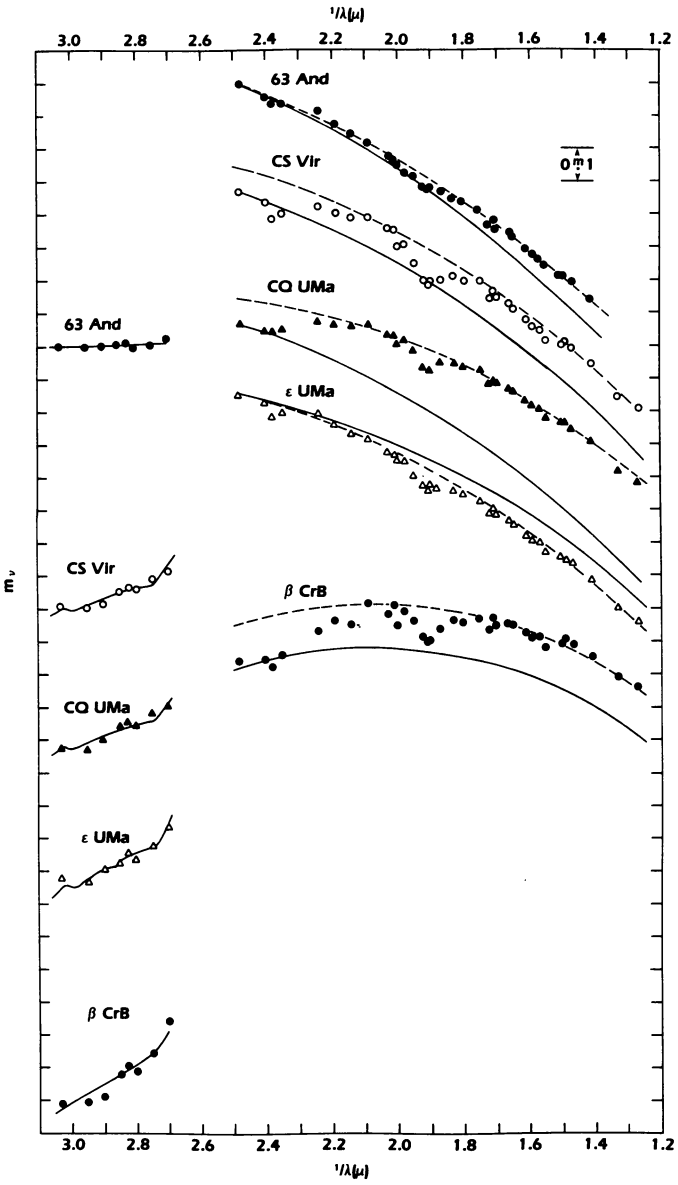

FIGURE 2. — The observed average energy distributions for five Ap stars : 63 And, CS Vir, CQ Uma, ε UMa and β CrB, compared to solar composition, log g = 4.0 model atmospheres that best match the Paschen continuum (dashed lines, Balmer continuum not shown) and the Balmer jump (solid lines). The effective temperatures of the models are : 63 And, BJ, 12900 K and PC, 10750 K ; CS Vir, BJ, 10500 K and PC, 9875 K ; CQ UMa, BJ, 10250 K and PC, 8650 K ; ε UMa, BJ, 9000 K and PC, 9500 K ; and β CrB, BJ, 8000 K and PC, 8000 K.

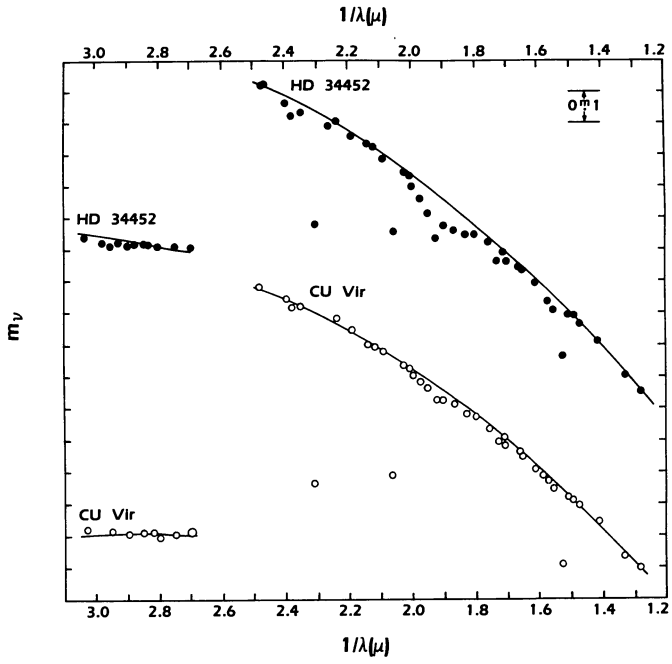

FIGURE 3. — The observed average energy distributions, normalized to λ5000, for HD 34452 and CU Vir, compared with solar composition, log g = 4.0 model atmospheres (solid lines) that give the best global match. The Hγ, Hβ and Hα values are shown but the predictions of the models in the region of the Balmer confluence of lines are not shown. The effective temperatures of the models are : HD 34452, 15800 K ; CU Vir, 13000 K.

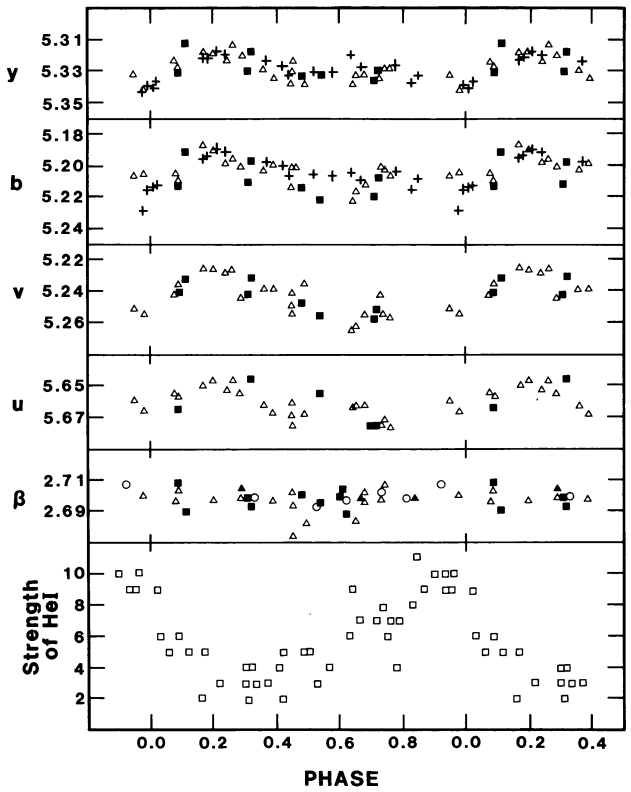

FIGURE 4. — Photometric variations of HD 34452 as a function of phase. Open triangles represent the four-color photometry of DMP and pluses, the photometry of Rakos (1962) (yellow and blue magnitudes on an instrumental system), the latter with an arbitrary magnitude shift. Closed triangles and closed squares represent spectrophotometric values of DMP/SJA and of REW in Paper VI, respectively. These values are : $m(5556)$, $m(4566)$, $m(4167)$ and $m(3509)$ in the y, b, v and u plots, respectively, and h and hb in the β plot. Open circles are the hb values of SJA and open squares are the He I line strengths of Deutsch (1947). All spectrophotometric values have arbitrary magnitude shifts.

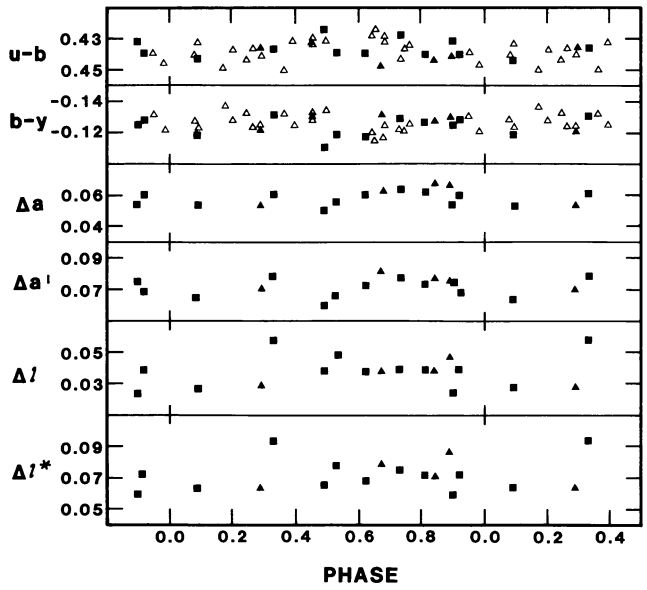

FIGURE 5. — The index values of HD 34452 as a function of phase. The symbols are the same as in figure 4.

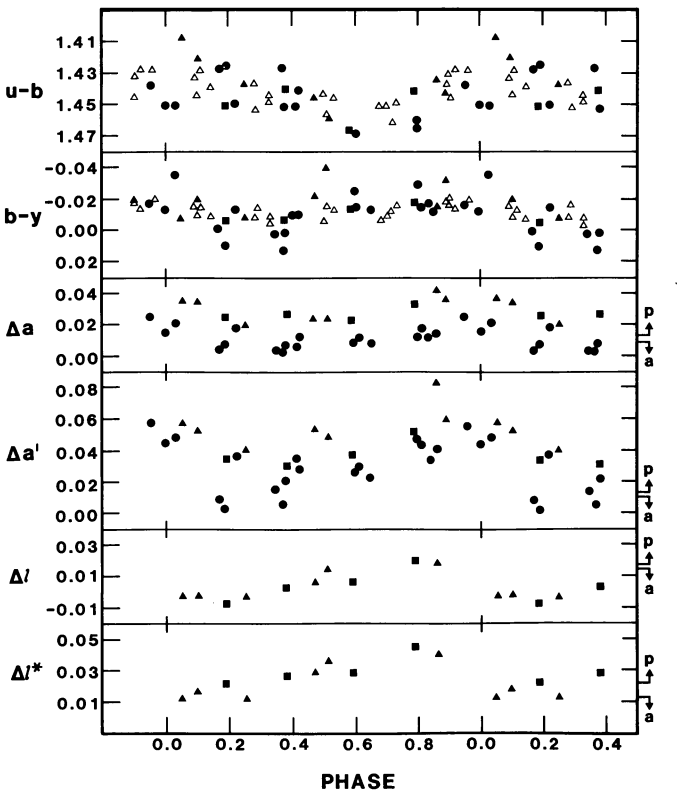

FIGURE 6. — The index values of ε UMa as a function of phase. Closed circles and closed squares represent the spectrophotometric values of DMP and SJA, respectively, the other symbols are the same as in figure 4.

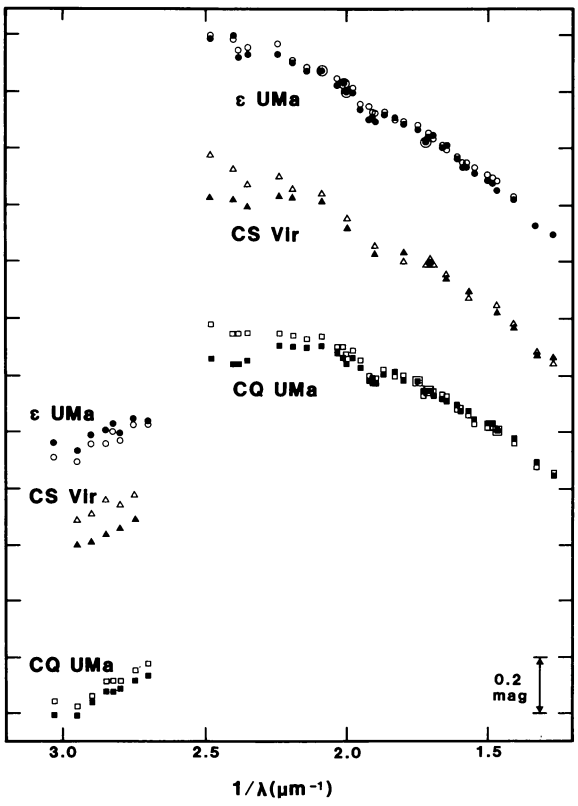

FIGURE 7. — Energy distributions of ε UMa, CS Vir and CQ UMa at the phases of their maximum differences in *b-y* and/or *u-b*. The ε UMa scans are normalized to λ5000, the others to λ5840. For ε UMa, the open circles represent scan 20 (phase 0.6) and the closed circles scan 27 (phase 0.0). For CS Vir, the open triangles are the averages of scans 2, 8 and 11 (phase 0.6) and the closed triangles the averages of scans 4, 9 and 10 (phase 0.0). For CQ UMa, the open squares are the averages of scans 4, 7, 10, 18 and 19 (phase 0.9) and the closed squares the averages of scans 11, 12 and 16 (phase 0.4).

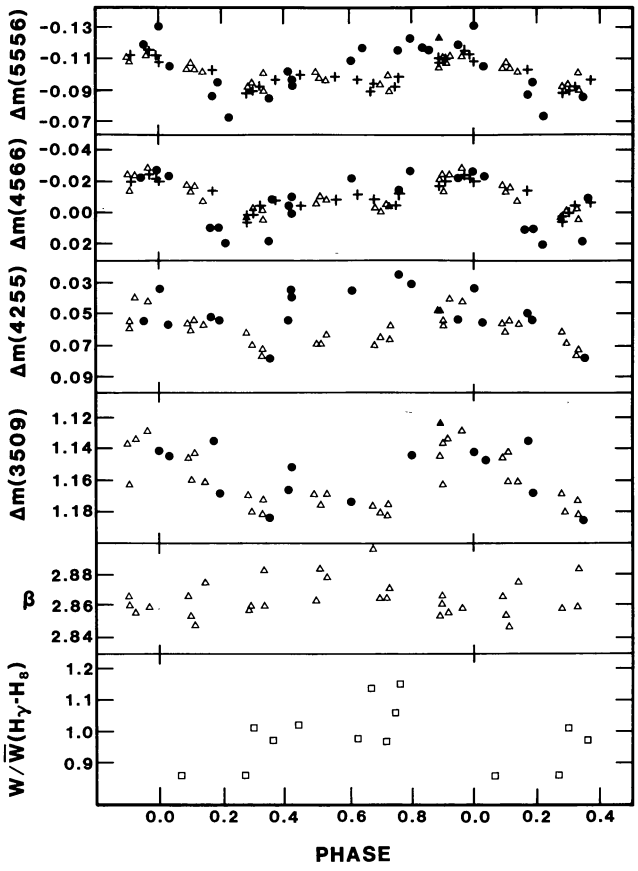

FIGURE 8. — Photometric variations of ε UMa as a function of phase. Pluses represent the photometry of Provin (1953), yellow and blue magnitudes in an instrumental system, respectively, in the top two plots. Open squares represent the equivalent widths of Woszczyk and Michalowski (1981), the other symbols are the same as in figure 6. The four-color *y*, *b*, *v* and *u* magnitudes are plotted in the top four plots, respectively. The scales are those of the spectrophotometry, the photometric values have arbitrary magnitude shifts.

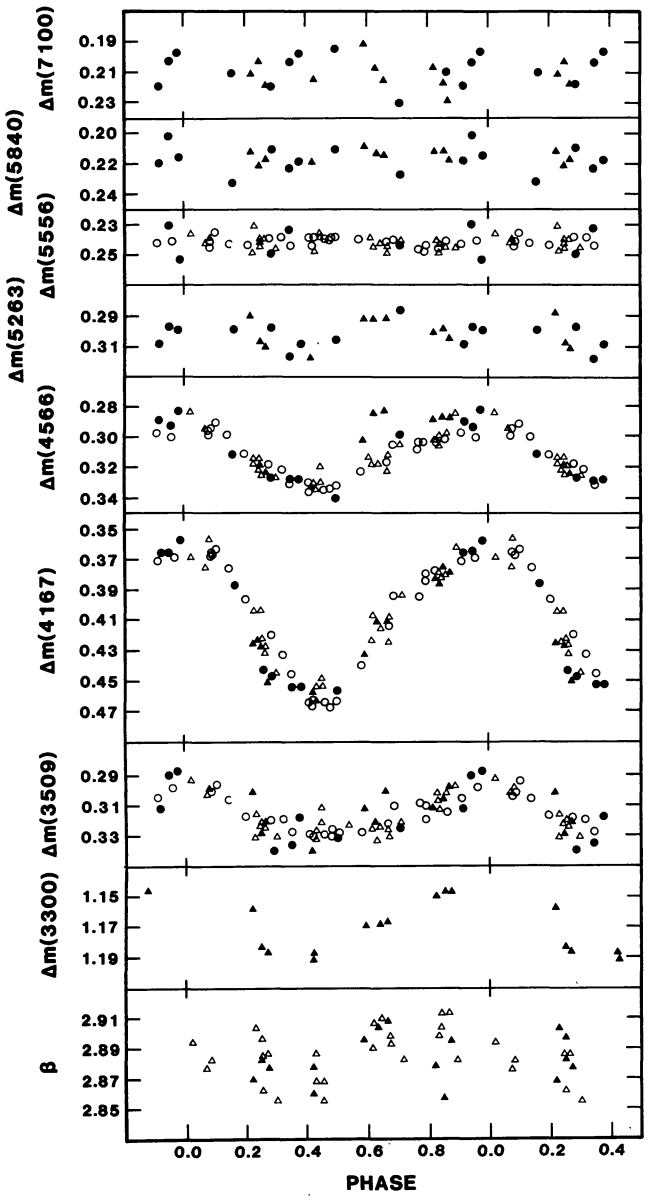

FIGURE 9. — Photometric variations of CQ UMa as a function of phase. Open circles represent the four-color photometry of Wolff and Morrison (1975), the other symbols are the same as in figure 6. The DMP/SJA values are $m(\lambda)$-m(5556) indices. The four-color y, b, v and u values are plotted in the Δm(5556), Δm(4566), Δm(4167) and Δm(3509) plots, respectively, with arbitrary magnitude shifts. In the bottom plot, the closed triangles are *hb* values, with an arbitrary magnitude shift.

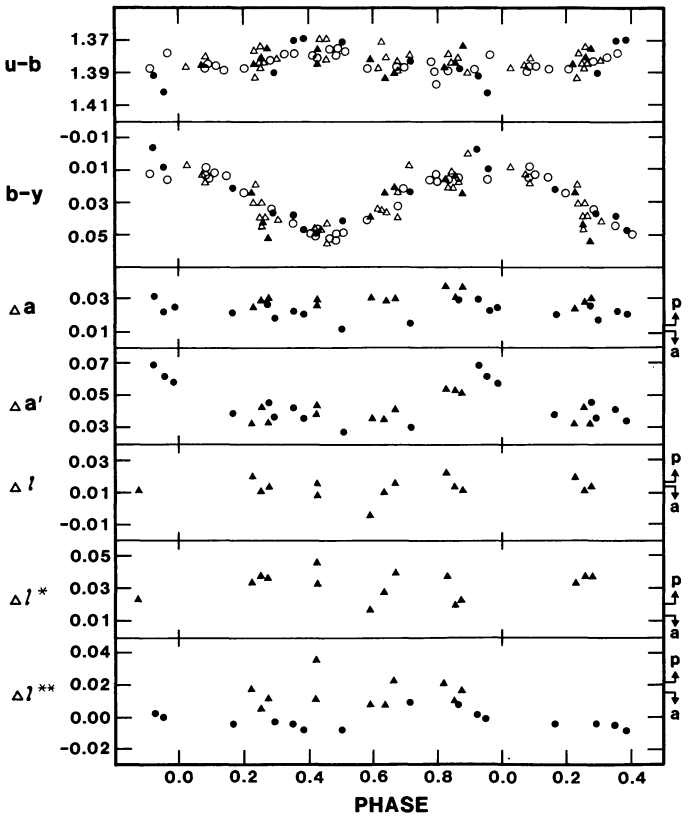

FIGURE 10. — The index values of CQ UMa as a function of phase. Symbols are the same as in figure 9.

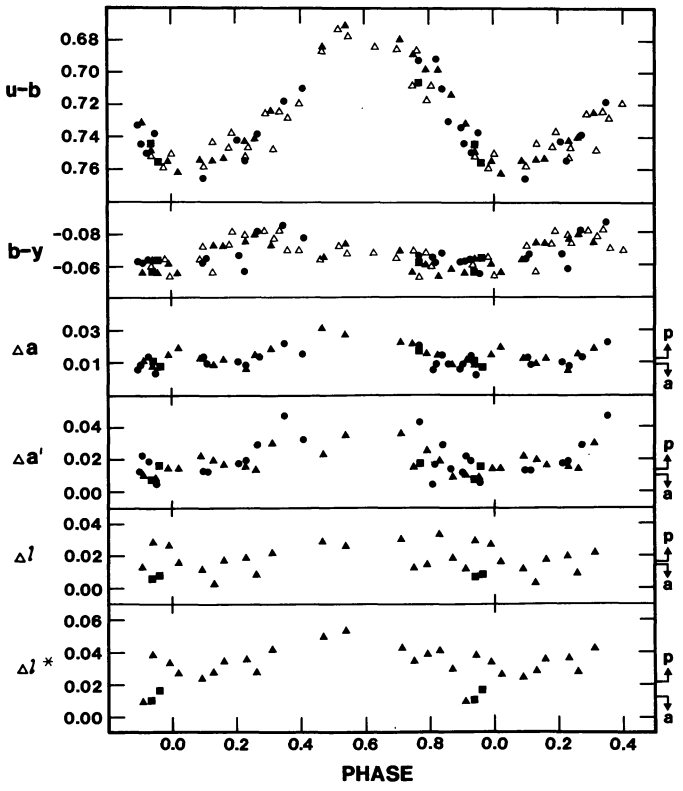

FIGURE 11. — Index values of CU Vir as a function of phase. The symbols are the same as in figure 6.

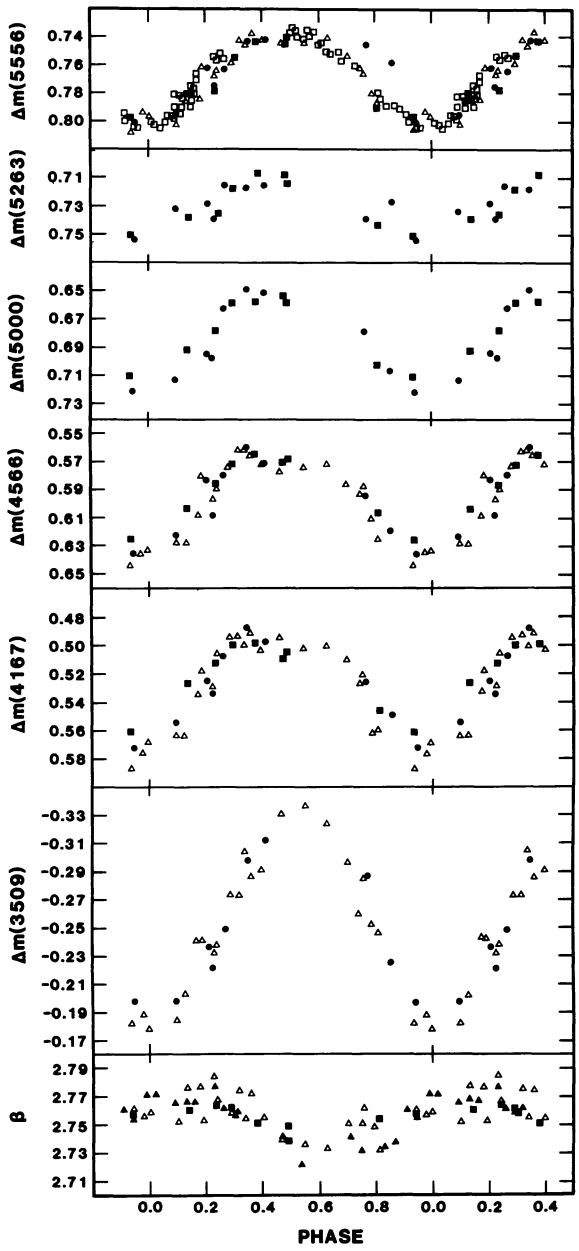

FIGURE 12. — Photometric variations of CU Vir as a function of phase. Open squares represent V values of Hardie (1958), and closed squares the $m(\lambda)$ spectrophotometric values of REW from Paper IV. Other symbols are the same as in figure 6. The V and y values are plotted in the $\Delta m(5556)$ plot, the b, v and u values in the $\Delta m(4566)$, $\Delta m(4167)$ and $\Delta m(3509)$ plots, respectively, all with arbitrary magnitude shifts. In the bottom plot, the closed triangles represent hb values and the closed squares h values, both with arbitrary magnitude shifts.

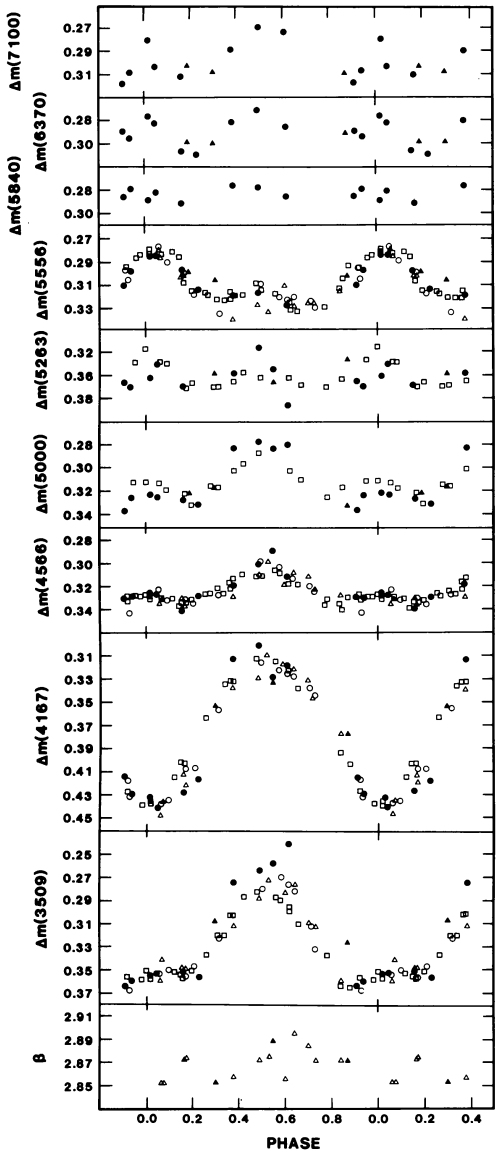

FIGURE 13. — Photometric variations of CS Vir as a function of phase. Open circles are the four-color values of Wolff and Wolff (1971) and open squares the four-color, g_1, g_2 photometry of Maitzen and Moffat (1972); the other symbols are the same as in figure 6. The y, g_2, g_1 b, v and u values are plotted in the $\Delta m(5556)$, $\Delta m(5263)$, $\Delta m(5000)$, $\Delta m(4566)$, $\Delta m(4167)$ and $\Delta m(3509)$ plots, respectively; in the β plot, the closed triangles are hb values. All photometric values have arbitrary magnitude shifts.

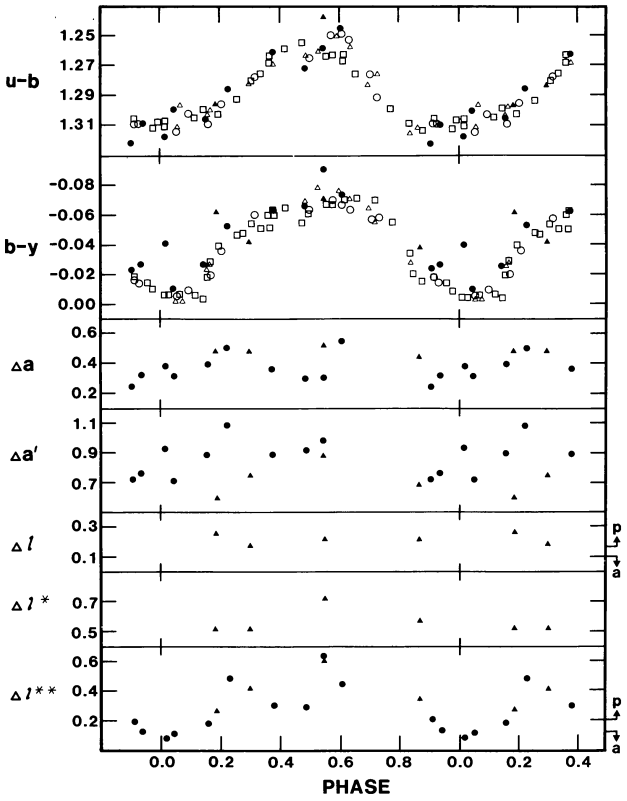

FIGURE 14. — Index values of CS Vir as a function of phase. Symbols are the same as in figure 13.

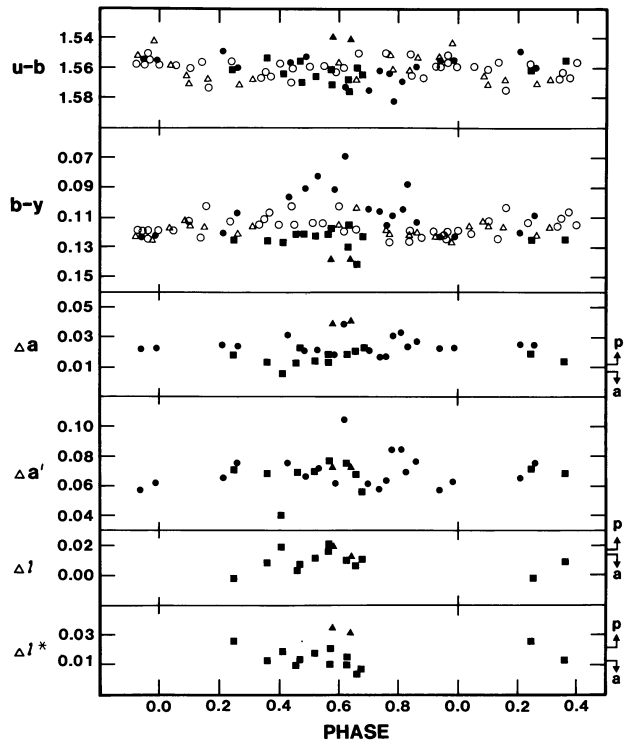

FIGURE 15. — Index values of β CrB as a function of phase. Closed squares are spectrophotometric values of SJA, other symbols are the same as in figure 13.

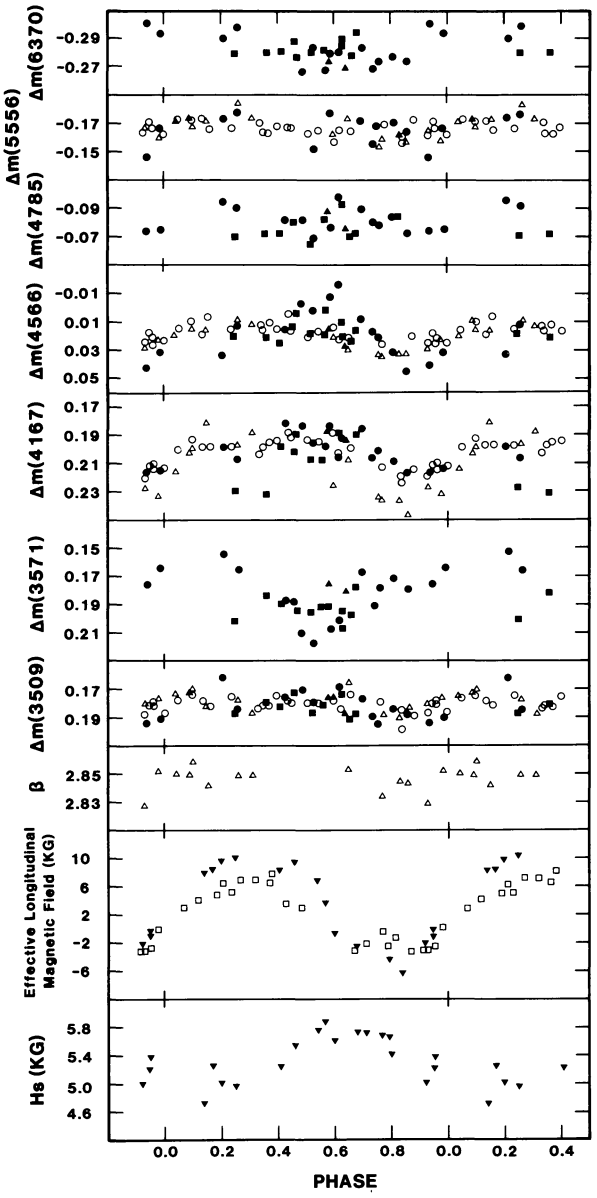

FIGURE 16. — Photometric variations of β CrB as a function of phase. Open squares represent the $B_{\rm eff}$ values of Borra and Landstreet (1980) and inverted closed triangles the $H_{\rm eff}$ and $H_{\rm s}$ values of Wolff and Wolff (1970). Other symbols are the same as in figure 13. All four-color magnitudes have arbitrary shifts.

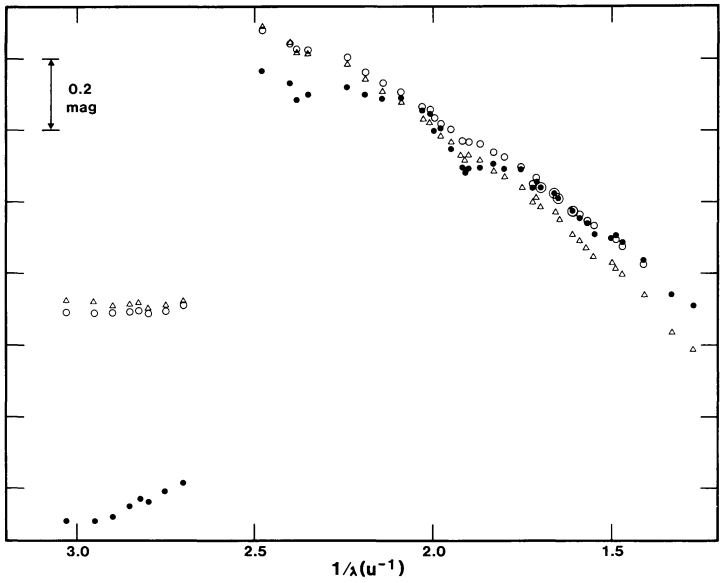

FIGURE 17. — Comparison of the average energy distributions of CU Vir (open triangles), 63 And (open circles) and CS Vir (closed circles). The values for CU Vir and CS Vir are normalized to λ5000, those for 63 And are shifted to match the red Paschen continuum of CS Vir.